

1 **Physiological and isotopic characteristics of nitrogen fixation by hyperthermophilic**
2 **methanogens: Key insights into nitrogen anabolism of the microbial communities in**
3 **Archean hydrothermal systems**

4

5 Manabu Nishizawa¹, Junichi Miyazaki^{1,2}, Akiko Makabe³, Keisuke Koba³ and Ken Takai^{1,2}6 ¹*Precambrian Ecosystem Laboratory (PEL)*7 ²*Subsurface Geobiology Advanced Research (SUGAR) Program*8 *Japan Agency for Marine-Earth Science and Technology (JAMSTEC), 2-15 Natsushima-cho,*
9 *Yokosuka 237-0061, Japan.*10 ³*Graduate School of Agriculture, Tokyo University of Agriculture and Technology, Tokyo, 183-8509,*
11 *Japan.*

12

13 Corresponding author: Manabu Nishizawa

14 E-mail: m_nishizawa@jamstec.go.jp; Phone: +81-46-867-9669; Fax: +81-46-867-9645

15

16 **Abstract**

17 Hyperthermophilic hydrogenotrophic methanogens represent one of the most important primary
18 producers in hydrogen (H₂)-abundant hydrothermal environments in the present-day ocean and
19 throughout the history of the Earth. However, the nitrogen sources supporting the development of
20 microbial communities in hydrothermal environments remain poorly understood. We have
21 investigated, for the first time, methanogenic archaea commonly found in deep-sea hydrothermal
22 environments to understand their physiological properties (growth kinetics, energetics, and metal
23 requirements) and isotopic characteristics during the fixation of dinitrogen (N₂), which is an
24 abundant but less-bioavailable compound in hydrothermal fluids. Culture experiments showed that
25 *Methanocaldococcus* strain (Mc 1-85N) (T_{opt} = 85 °C) and *Methanothermococcus* strain (Mt 5-55N)
26 (T_{opt} = 55 °C) assimilated N₂ and ammonium, but not nitrate. Previous phylogenetic studies have
27 predicted that the *Methanocaldococcus* and *Methanothermococcus* lineages have nitrogenases, key
28 enzymes for N₂ fixation, with biochemically uncharacterised active site metal cofactors. We showed
29 that Mt 5-55N required molybdenum for the nitrogenase to function, implying a
30 molybdenum-bearing cofactor in the strain. Molybdenum also stimulated diazotrophic (i.e.,
31 N₂-fixing) growth of Mc 1-85N, though further experiments are required to test whether the strain
32 contains a molybdenum-dependent nitrogenase. Importantly, Mc 1-85N exhibited an apparently
33 lower requirement of and higher tolerance to molybdenum and iron than Mt 5-55N. Furthermore,
34 both strains produced more ¹⁵N-depleted biomass (-4‰ relative to N₂) than that previously reported
35 for diazotrophic photosynthetic prokaryotes. These results demonstrate that diazotrophic
36 hyperthermophilic methanogens can be broadly distributed in seafloor and subseafloor hydrothermal
37 environments, where the availability of transition metals is variable and where organic carbon,
38 organic nitrogen, and ammonium are generally scarce. The emergence and function of diazotrophy,
39 coupled with methanogenesis, in the early Earth is also consistent with the nitrogen isotopic records
40 of 3.5 billion-year-old hydrothermal deposits.

41

42 **Keywords:** nitrogen fixation, ammonium assimilation, nitrogen fixation rate, metal requirements,
43 isotopic systematics, methanogen, nitrogen cycle, early Earth

44

45 1. Introduction

46 Deep-sea hydrothermal systems provide a variety of microbial habitats, and the focused and
47 diffusing hydrothermal fluids contain microorganisms from reduced hot subseafloor environments
48 (Deming and Baross, 1993; Summit and Baross, 1998; Takai and Nakamura, 2010; 2011).
49 Microbiological and chemical components entrained in the discharging hydrothermal fluids and
50 included in the subseafloor fluids are key signals for understanding the composition and function of
51 indigenous microbial communities living in the subseafloor (Karl et al., 1989; Cowen et al., 2003;
52 Butterfield et al., 2004; Takai et al., 2004; Orcutt et al., 2011). Many hyperthermophilic (optimal
53 growth temperature: 70-120 °C) and thermophilic (optimal growth temperature: 50-70 °C)
54 microorganisms have been isolated from seafloor hydrothermal environments, and these
55 microorganisms utilise a variety of energy, carbon and nitrogen sources (e.g., Jones et al., 1983;
56 Neuner et al., 1990; Huber et al., 1992; Nakagawa et al., 2003). Thermodynamic calculations and
57 microbial community compositions in the hydrothermal mixing zones suggest that the
58 chemolithotrophic energy potentials obtained from the hydrothermal fluids and the ambient seawater
59 would control the development of chemolithotrophic microbial communities associated with
60 hydrothermal activities (McCollom and Shock, 1997; Shock and Holland, 2004; Tivey et al., 2004;
61 Takai and Nakamura, 2010; 2011). In addition to the chemolithotrophic energy state, the abundance
62 and availability of biologically essential elements, such as nitrogen, phosphorus and transition metals,
63 would significantly affect the composition and function of the microbial communities (Takai and
64 Nakamura, 2010). However, the nitrogen sources supporting the development of chemolithotrophic
65 microbial communities in the seafloor and subseafloor hydrothermal environments remain poorly
66 understood.

67 The nitrate (NO_3^-) concentration in diffusing hydrothermal fluids (< 120 °C) is generally lower
68 than that expected from a simple mixing of a magnesium-zero end-member hydrothermal fluid (0
69 μM) and the ambient deep-sea water (40 μM) (Johnson et al., 1988; Karl et al., 1989; Bourbonnais et
70 al., 2012a). For instance, the nitrate concentration is less than 20 μM in the low-temperature (20 °C)
71 diffusing fluids of the Galapagos spreading centre (Johnson et al., 1988). The non-conservative
72 nitrate depletion most likely originates from biological consumption because many microorganisms
73 can utilise nitrate via assimilatory and/or dissimilatory reduction (Nakagawa et al., 2003; Nakagawa

74 et al., 2005; Bourbonnais et al., 2012b). Nitrogen isotopic ratios of the nitrate in the diffusing fluids
75 have been reported only from the Juan de Fuca Ridge, and they seem to increase from 6‰ (the value
76 of nitrate in deep-sea water) to 10‰ as the degree of non-conservative nitrate depletion increases
77 (Bourbonnais et al., 2012a). The ammonium (NH_4^+) concentration in high temperature ($> 150\text{ }^\circ\text{C}$)
78 hydrothermal fluids in unsedimented systems is typically similar to that of the ambient deep-sea
79 water ($1\text{ }\mu\text{M}$ or less), but it is occasionally as high as $15\text{ }\mu\text{M}$ in certain fields (German and Von
80 Damm, 2003; Bourbonnais et al., 2012a). The exception is hydrothermal fluids ($> 300\text{ }^\circ\text{C}$) venting
81 from the Endeavour Segment on the Juan de Fuca Ridge, where decomposition of organic matter in
82 sediments buried at an early stage of the ridge formation has been proposed to be the candidate
83 source of ammonium ($1000\text{ }\mu\text{M}$, Lilley et al., 1993; Bourbonnais et al., 2012a). Nitrogen isotopic
84 ratios of ammonium in hydrothermal fluids have been reported only from the Juan de Fuca Ridge,
85 and they are $6.7 \pm 1.0\text{‰}$ ($n = 16$) at the Axial Volcano and $3.7 \pm 0.6\text{‰}$ ($n = 37$) at the Endeavour
86 Segment (Bourbonnais et al., 2012a). Dissolved dinitrogen (N_2) is more abundant in hydrothermal
87 fluids than nitrate and ammonium ($400\text{--}3400\text{ }\mu\text{M}$ in magnesium-zero end-member hydrothermal
88 fluids and $590\text{ }\mu\text{M}$ in deep-sea water) (Charlou et al., 1996; 2000; 2002). Isotopic ratios of N_2 in
89 hydrothermal fluids have been reported only from the Tonga-Kermadec Arc, and they are slightly
90 depleted in ^{15}N relative to deep-sea water (0‰) by 2‰ (de Ronde et al., 2011).

91 Previous studies have shown that a limited number of hyperthermophilic and thermophilic
92 microorganisms can assimilate N_2 via a nitrogenase enzyme complex that catalyses N_2 reduction to
93 ammonia (diazotrophy) (Belay et al., 1984; Mehta and Baross, 2006; Steunou et al., 2006; Hamilton
94 et al., 2011). Furthermore, the phylogenetic diversity of nitrogenase genes (*nifH*) in deep-sea
95 hydrothermal fluids has pointed to the presence of methanogenic archaea and anaerobic bacteria
96 (clostridia, sulphate-reducing proteobacteria) as potential nitrogen fixers in the seafloor microbial
97 communities (Mehta et al., 2003).

98 The discovery of diazotrophic hyperthermophilic methanogens (Mehta and Baross, 2006) has
99 highlighted the potential ubiquity and important role of these organisms in H_2 -abundant marine
100 hydrothermal environments throughout Earth history. Hyperthermophilic methanogens represent one
101 of the most predominant primary producers in the deep-sea hydrothermal environments with
102 hydrothermal fluid chemistries that are characterised by highly enriched H_2 (more than
103 approximately 1 mM) (Takai et al., 2004; Flores et al., 2011). Furthermore, hyperthermophilic

104 methanogenesis has been theoretically and empirically predicted as one of the most ancient
105 chemolithotrophic energy metabolisms supporting the earliest ecosystem associated with the ocean
106 hydrothermal systems on the Hadean Earth (Russell and Martin, 2004; Ferry and House, 2006; Takai
107 et al., 2006; Sleep and Bird, 2007; Martin et al., 2008; Russell et al., 2010). In fact, geological
108 evidence of ancient methanogenesis in seafloor and subseafloor hydrothermal environments has been
109 furnished by hydrothermal deposit records that date to 3.5 billion years ago (giga-annum, Ga) (Ueno
110 et al., 2006).

111 Although many studies have reported on the ecophysiology and biochemistry of
112 methanogenesis metabolisms and functions (Garcia et al., 2000; Thauer et al., 2008), the physiology
113 of nitrogen fixation in hyperthermophilic methanogens remains to be elucidated, including the rate
114 and energetics of nitrogen fixation and the biological requirement of transition metals used in the
115 nitrogenase cofactors (e.g., molybdenum (Mo) and iron (Fe)). In addition, the isotopic systematics of
116 nitrogen fixation in hyperthermophilic methanogens should be investigated to explain the role of the
117 global biogeochemical nitrogen cycle throughout Earth's history.

118 In the present-day ocean, more than 70% of biological nitrogen compounds are provided by
119 microbial nitrogen fixation ($1-3 \times 10^{14}$ gN/y) (Brandes and Devol, 2002). By contrast, on the early
120 Earth, the potential nitrogen sources for living forms should have been produced by abiotic processes,
121 such as atmospheric production of nitric oxide by lightning (Navarro-González et al., 2001),
122 photochemical production of hydrogen cyanide (Zahnle et al., 1986), multistep conversion of nitric
123 oxide and hydrogen cyanide to ammonium in the ocean (Zahnle et al., 1986; Summers and Chang et
124 al., 1993; Brandes et al., 1998; Summers 2005; Brandes et al., 2008; Singireddy et al., 2012), shock
125 synthesis of amines and amino acids (Furukawa et al., 2008), and hydrothermal synthesis of
126 ammonia from N₂ reduction (Brandes et al., 1998, Schoonen and Xu, 2001; Smirnov et al., 2008).
127 These prebiotic sources of biologically available nitrogen may have been sufficient immediately after
128 the origin of life, but such abiotically produced nitrogen pools were likely drained by the early
129 expansion of microbial populations and habitats. This process may have triggered the onset of
130 biological nitrogen fixation. Based on the phylogenetic analyses of nitrogenase sequences, two
131 possible hypotheses for the origin of nitrogen fixation have been proposed (Leigh, 2000; Raymond et
132 al., 2004; Boyd et al., 2011b). One hypothesis proposes that the Mo-Fe-type nitrogenase was present
133 in the last universal common ancestor (LUCA origin model) (Leigh, 2000; Raymond et al., 2004),

134 whereas the other claims that the Mo-Fe-type nitrogenase was derived from the ancestral
135 methanogens (methanogen origin model) (Boyd et al., 2011b). To trace the time and place of the
136 possible onset of biological nitrogen fixation, researchers have used not only an approach based on
137 molecular evolution but also an approach involving the exploration of chemical fossils (isotopic
138 signatures) in the geological record (Beaumont and Robert, 1999; Nishizawa et al., 2007). However,
139 because the isotopic characteristics of nitrogen fixation in methanogens have, until now, been
140 completely unknown, the interpretation of the geological record has been equivocal.

141 We report, for the first time, the physiological properties and isotopic characteristics of
142 nitrogen anabolisms, including nitrogen fixation, in hyperthermophilic and thermophilic
143 methanogenic genera found in global hydrothermal environments (*Methanocaldococcus* and
144 *Methanothermococcus* spp.) (Takai et al., 2004; Flores et al., 2011; Ver Eecke et al., 2012). These
145 methanogens, together with anaerobic archaeal methanotrophs, are known to encode for nitrogenase
146 homologs that do not cluster phylogenetically with previously characterised nitrogenases with
147 iron-molybdenum (FeMo), iron-vanadium (FeV) or iron-iron (FeFe) cofactors (Dekas et al., 2009;
148 Boyd et al., 2011a; Dos Santos et al., 2012). Cultivation experiments were conducted under various
149 conditions (e.g., under varying concentrations of Mo, Fe, N₂ and H₂ in the culture media) to
150 potentially reproduce present and past oceanic and hydrothermal environments. The results include
151 the novel finding that diazotrophic methanogens produce biomass that is more depleted in ¹⁵N than
152 diazotrophic photosynthetic prokaryotes (Minagawa and Wada, 1986; Macko et al., 1987; Carpenter
153 et al., 1997; Beaumont et al., 2000; Zerkle et al., 2008; Bauersachs et al., 2009). The relatively large
154 isotopic fractionation effect of the methanogens and its evolutionary implications are also discussed.

155

156 **2. Methods**

157 **2-1. Isolation and phylogenetic characterisation of methanogenic strains**

158 We used two strains of hyperthermophilic and thermophilic methanogens isolated from the
159 Kairei field on the Central Indian Ridge. A hyperthermophilic methanogen was isolated from an *in*
160 *situ* cultivation system (ISCS) deployed in 362 °C black smoker fluid from the Kali chimney at the
161 Kairei Field. A slurry sample of the ISCS substratum was inoculated into a nitrogen-fixing medium
162 (see section 2-2 for the chemical composition) prepared in test tubes with a gas phase of N₂ (0.1

163 MPa), CO₂ (0.1 MPa) and H₂ (0.2 MPa). A positive enrichment culture was obtained from the test
164 tube incubated at 85 °C, and coccoid cells with F420-dependent autofluorescence were observed.
165 Similarly, a thermophilic methanogen was isolated from an outer portion of the Kali chimney
166 structure. The chimney sample was inoculated into a nitrogen-fixing medium prepared in test tubes
167 with a gas phase of N₂ (0.1 MPa), CO₂ (0.1 MPa) and H₂ (0.2 MPa). A positive enrichment culture
168 was obtained from the test tube incubated at 55 °C, and coccoid cells with F420-dependent
169 autofluorescence were observed. The dilution-to-extinction method (Takai et al., 2008) was used to
170 purify these strains using the same medium at 85 and 55 °C, respectively. A phylogenetic analysis of
171 the 16S rRNA gene sequences revealed that the strain grown at 85 °C belonged to the genus
172 *Methanocaldococcus* and was closely (99% similarity) related to a strain of *Methanocaldococcus*
173 FS406-22. The analysis also showed that the strain grown at 55 °C belonged to the genus
174 *Methanothermococcus* and was closely (99% similarity) related to a strain of *Methanothermococcus*
175 okinawensis. We assigned the name *Methanocaldococcus* sp. kairei 1-85N (grown at 85 °C)
176 (described as Mc 1-85N hereafter) to the former strain and the name *Methanothermococcus* sp. kairei
177 5-55N (grown at 55 °C) (described as Mt 5-55N hereafter) to the latter strain. Nitrogen fixation by
178 Mc 1-85N and Mt 5-55N was verified by uptake of ¹⁵N-labelled N₂ into cellular nitrogen under
179 cultivation with ¹⁵N-labelled N₂ as the sole nitrogen source.

180 **2-2. Medium preparation**

181 We conducted the diazotrophic cultivation of the methanogens in a nitrogen-fixing medium. The
182 medium contained (g per litre): NaCl, 30; KH₂PO₄, 0.09; K₂HPO₄, 0.09; MgCl₂/6H₂O, 3.0;
183 MgSO₄/7H₂O, 4.0; CaCl₂, 0.8; KCl, 0.33; NiCl₂, 0.002; Na₂SeO₃, 0.002. A solution of trace minerals
184 (10 mL) was added to a litre of the medium. The trace mineral solution contained (g per litre):
185 MgSO₄/7H₂O, 3; MnSO₄/H₂O, 0.5; CoSO₄/7H₂O, 0.18; CaCl₂/2H₂O, 0.1; ZnSO₄/7H₂O, 0.18;
186 CuSO₄/5H₂O, 0.01; KAl(SO₄)₂/12H₂O, 0.02; H₃BO₃, 0.01; NiCl₂/6H₂O, 0.025; Na₂SeO₃/5H₂O,
187 0.0003. Subsequently, 20 mL of the medium was dispensed into a 160-mL glass serum bottle and
188 autoclaved at 121 °C for 20 min. Na₂MoO₄ and FeCl₃ solutions (filter-sterilised) were then added to
189 the medium on a clean bench. In the basic experiment, the gas phase consisted of N₂ (0.1 MPa), CO₂
190 (0.1 MPa) and H₂ (0.2 MPa). The medium was buffered with 12 mM NaHCO₃ solution
191 (filter-sterilised) to a final pH of 6.0 (at room temperature) and was reduced by the addition of

192 Na₂S/9H₂O solution to a final concentration of 2.1 mM. The glass bottle was sealed with a sterile
193 butyl rubber stopper and crimped with an aluminium seal. The concentration of ammonium
194 incorporated as an impurity of the medium and a carryover in the inoculum was less than 5 µM, and
195 the concentration of ammonium after diazotrophic cultivation was generally less than 6 µM. For
196 comparison purposes, a negative control experiment was conducted under a gas phase of Ar (0.1
197 MPa), CO₂ (0.1 MPa) and H₂ (0.2 MPa). Additionally, a series of ammonium-supplemented
198 cultivation experiments was conducted by adding NH₄Cl (100 µM–10 mM) to the medium. The gas
199 phase consisted of Ar (0.1 MPa), CO₂ (0.1 MPa) and H₂ (0.2 MPa) or N₂ (0.1 MPa), CO₂ (0.1 MPa)
200 and H₂ (0.2 MPa) when the initial concentration of the ammonium in the medium was 10 mM. By
201 contrast, the gas phase consisted of CO₂ (0.1 MPa) and H₂ (0.2 MPa) when the initial concentration
202 of the ammonium was below 1 mM (i.e., 100, 200, 1000 µM).

203 In a growth experiment under high-pressure, 5 mL or 10 mL of the medium was dispensed into
204 a 30 mL Sulfinert-coated stainless steel tube (Swagelok, Ohio) with an instrument plug valve capable
205 of operating up to 413 bar and 121 °C. The headspace was replaced by N₂ (2 MPa), CO₂ (0.1 MPa)
206 and H₂ (2 MPa). The final concentrations of NaHCO₃ and Na₂S/9H₂O were adjusted to 12 mM and
207 2.1 mM, respectively.

208

209 **2-3. Cultivation experiments**

210 We pre-cultured the methanogen strains under the same conditions as those of the designed
211 cultivation experiment and inoculated the strains into fresh media. The cultivation temperatures were
212 85 °C for Mc 1-85N and 55 °C for Mt 5-55N. The duration of the cultivations ranged from 9.5 to 43
213 hours. We estimated the initial concentrations of the gaseous components dissolved in the media are
214 1.3 mM (H₂) and 0.4 mM (N₂) in the basic experiments and 13 mM (H₂) and 8 mM (N₂) in the
215 high-pressure experiments (Wiesenburg and Guinasso 1979). The measured pH values of the media
216 during cultivation always ranged from 5.7 to 6.1. The Mo speciation in sulphidic water was
217 experimentally investigated at 25 °C, and most of the Mo (VI) (99.9% or more) was found to exist as
218 oxythiomolybdate (MoO_{4-x}S_x²⁻) at a neutral pH with 0.5 mM H₂S (Erickson and Helz, 2000).
219 Although there is no study on Mo speciation in sulphidic water at high temperatures, most of the Mo
220 in our media would likely exist as oxythiomolybdate under the experimental conditions. The growth

221 was tracked by direct counting of DAPI-stained cells. The uncertainty associated with the cell counts
222 was estimated to be 20-30% (one standard deviation) through replicate measurements.

223

224 **2-4. Chemical and isotopic analyses**

225 To investigate the isotopic characteristics of nitrogen fixation, the concentrations and isotopic
226 compositions of particulate nitrogen (PN) and total nitrogen (TN: sum of PN and dissolved nitrogen
227 compounds, except for N₂) were analysed for Mc 1-85N and Mt 5-55N. After cultivation, the
228 particulate matter (primarily cells) in the medium was collected by filtration through a GF/F filter
229 (pre-combusted at 450 °C for 4 h). Subsequently, the amount and the isotopic ratio of PN were
230 measured by combustion of the GF/F filter at 1,000 °C in a FLASH EA 1112 elemental analyser on
231 line with a Finnigan DELTAplus Advantage mass spectrometer at JAMSTEC. The precision
232 achieved with repeated analyses of in-house standards (alanine, glycine, and histidine) was typically
233 greater than 10% for the PN concentration and greater than 0.4‰ for δ¹⁵N. The PN concentration
234 should be considered a minimum estimate because it is possible that some fractions of the particulate
235 matter passed through the GF/F filter (Hewson et al., 2004).

236 To measure the concentration and isotopic ratio of TN, the TN in the medium was converted to
237 N₂O via two reaction steps. First, the TN was converted to nitrate by the persulphate oxidation
238 method, and the resulting nitrate was then converted to N₂O by the denitrifier method (Koba et al.,
239 2010). After purification by gas chromatography (Agilent HP6890) with a Poraplot column (25 m ×
240 0.32 mm), the concentration and isotopic ratio of the resultant N₂O were analysed with a Finnigan
241 DELTAplus XP mass spectrometer at the Tokyo University of Agriculture and Technology
242 (Nishizawa et al., 2013). The overall precision achieved with repeated analyses of the same sample
243 was typically 10% for the TN concentration and greater than 0.7‰ for δ¹⁵N. The nitrogen isotopic
244 ratios of PN and TN were expressed as δ¹⁵N relative to the substrate used in the cultivation (N₂ in the
245 diazotrophic condition, NH₄Cl in the non-diazotrophic condition). The δ¹⁵N value of the N₂ substrate
246 relative to air was -14.15 ± 0.05‰ (n = 2). This value was determined before the cultivation
247 experiment by a Finnigan MAT253 mass spectrometer in dual-inlet mode. The δ¹⁵N value of the
248 NH₄Cl substrate relative to air was -5.8 ± 0.4‰ (8.4‰ relative to the N₂ substrate; n = 7), as
249 determined by the online combustion method described above.

250 The ammonium concentration in the medium was determined by the indophenol blue method
 251 (reproducibility: $\pm 5\%$) (Solorzano 1969). The methane (CH₄) concentration in the headspace was
 252 measured by gas chromatography coupled with a thermal conductivity detector (GC-TCD,
 253 reproducibility: $\pm 2\%$) (GL Science GC-3200). The total Fe and Mo concentrations in the medium
 254 were measured with ICP-MS (internal precision: better than 5%) (Agilent 7500ce).

255

256 2-5. Calculations

257 The cell-specific growth rate was calculated from the slope of the growth curve in exponential
 258 phase and was reported as μ (h⁻¹). The cell-specific nitrogen uptake rate in the exponential phase, ρN
 259 (mol N \times cell⁻¹ \times min⁻¹), was calculated from the relation $\rho\text{N} = \mu \times Q_{\text{N}}$ (eq. 1), where Q_{N} denotes
 260 cellular nitrogen content (mol N \times cell⁻¹) (Tuit et al., 2004). The ρN was determined from replicate
 261 experiments ($n = 3-7$).

262 The amount of chemical energy potentially available to the methanogen was calculated from the
 263 change in the Gibbs free energy associated with methanogenesis ($4\text{H}_2(\text{aq}) + \text{CO}_2(\text{aq}) \rightarrow \text{CH}_4(\text{aq}) +$
 264 $2\text{H}_2\text{O}$). We used the following equation: Potential energy yield = $RT * \ln(K/Q)$ (eq. 2). R is the
 265 universal gas constant, T is the temperature in Kelvin, and K represents the equilibrium constant,
 266 which is calculated from the standard Gibbs free energy of methanogenesis (ΔG°_r) at the cultivation
 267 temperature and pressure, using the relation $\Delta G^{\circ}_r = -RT * \ln K$. The activity product Q was
 268 calculated from the relation $Q = a_{\text{CH}_4} / (a_{\text{CO}_2} * a_{\text{H}_2}^4)$. The symbols a_{CH_4} , a_{CO_2} and $a_{\text{H}_2}^4$, respectively,
 269 denote the activities of CH₄, CO₂ and H₂ dissolved in the medium and were calculated from molar
 270 concentrations (m) and activity coefficients (γ) ($a = m * \gamma$). The amounts of H₂ and ΣCO_2 (sum of
 271 gaseous CO₂, aqueous CO₂, HCO₃⁻ and CO₃²⁻) consumed during our experiment were calculated
 272 from the measured amount of CH₄ produced. We neglected the contribution of cellular carbon to the
 273 amount of ΣCO_2 consumed due to the low amount of cellular carbon produced from ΣCO_2 (less than
 274 1.4%). Solubility of H₂ and CH₄ in the medium was calculated from Wiesenburg and Guinasso
 275 (1979). Values of ΔG°_r , γ , and CO₂ speciation in the medium during experiment (ionic strength =
 276 0.65 M) were calculated using the Geochemist's Workbench computer code (Bethke, 2008).

277 The isotopic ratio of TN produced during the growth of methanogens ($\delta^{15}\text{N}$ (TN pro.)) was
 278 calculated using the following equation: $\delta^{15}\text{N}$ (TN pro.) = $([\text{TN}] \times \delta^{15}\text{N} (\text{TN}) - [\text{TN}]' \times \delta^{15}\text{N} (\text{TN})') /$

279 $([TN] - [TN]')$ (eq. 3). Symbols $[TN]$ and $[TN]'$ denote concentrations of TN at T and T' hours after
 280 cultivation starts ($T > T'$).

281 The isotope enrichment factors ($\epsilon_{P/S}$) of nitrogen fixation and ammonium uptake were
 282 calculated using the following equation: $\delta^{15}N_{P,ac} = \delta^{15}N_{S,0} - f \times \ln(f) \times (1 - f)^{-1} \times \epsilon_{P/S}$ (eq. 4)
 283 (Mariotti et al., 1981). The $\delta^{15}N_{P,ac}$ and $\delta^{15}N_{S,0}$ symbols denote the nitrogen isotopic ratios of
 284 accumulated product (TN for the nitrogen fixation experiment and PN for the ammonium uptake
 285 experiment) and substrate (N_2 for the nitrogen fixation experiment and NH_4Cl for the ammonium
 286 uptake experiment), respectively. The symbol “f” denotes the remaining fraction of substrate. In the
 287 ammonium uptake experiment, the f value was calculated from the ammonium concentrations in the
 288 medium before and after cultivation. By contrast, equation 4 can be approximated by $\delta^{15}N_{P,ac} =$
 289 $\delta^{15}N_{S,0} + \epsilon_{P/S}$ in the nitrogen fixation experiment if the f value is greater than 0.98 (eq. 5).

290

291 **3. Results**

292 **3-1. Rates and metal requirements of nitrogen fixation**

293 Both Mc 1-85N and Mt 5-55N utilised N_2 and ammonium as the sole nitrogen source, but not
 294 nitrate (Figures 1a, b; Table 1). The diazotrophic growth of Mc 1-85N was observed in the presence
 295 of broad ranges of Mo and Fe concentrations (Mo = 5 nM–1 mM; Fe = 100 nM–10 mM) (Figure 1a
 296 and Table 1). In the media with higher Mo concentrations (10–1,000 μM), growth followed a simple
 297 exponential curve until the H_2 was largely consumed. In the media with lower Mo concentrations (5
 298 nM to 1 μM), growth initially followed a simple exponential curve and then reached the stationary
 299 phase before H_2 was depleted. Thus, it is likely that diazotrophic growth is directly linked to the
 300 availability of Mo in the medium.

301 Under the diazotrophic growth condition with a Fe concentration of 1 mM or less in the medium,
 302 the cell-specific growth rate in the exponential growth phase was almost constant ($0.28 \pm 0.03 \text{ h}^{-1}$, n =
 303 12), irrespective of the Mo concentrations added, but it was five times lower than that under the
 304 non-diazotrophic growth condition in the presence of 10 mM of ammonium (1.5 h^{-1}).

305 By contrast, Mt 5-55N exhibited diazotrophic growth under narrower ranges of Mo and Fe
 306 concentrations in the media (Mo = 1 μM –10 μM ; Fe = 10 μM –100 μM) (Figure 1b and Table 1).
 307 Interestingly, Mt 5-55N grew well at a low Mo concentration (Mo = 5 nM; Fe = 100 μM) (Table 1)

308 in the presence of 1 mM ammonium, which is an Mo concentration where the diazotrophic growth of
 309 Mt 5-55N was prevented. This result indicated that Mt 5-55N requires relatively higher amounts of
 310 Mo to activate its nitrogenase function. The specific growth rate in the exponential growth phase was
 311 $0.27 \pm 0.02 \text{ h}^{-1}$ in the diazotrophic growth condition, which was similar to that of Mc 1-85N.

312 The cell-specific nitrogen uptake rates in the exponential growth phase were estimated to be
 313 $2.11 \times 10^{-17} \text{ mol N} \times \text{cell}^{-1} \times \text{min}^{-1}$ for Mc 1-85N ($n = 7$) and $8 \times 10^{-17} \text{ mol N} \times \text{cell}^{-1} \times \text{min}^{-1}$ for Mt
 314 5-55N ($n = 2$), (cells = 1 μm in diameter for both strains) under the diazotrophic growth condition.
 315 The cell-specific nitrogen uptake rates of Mc 1-85N and Mt 5-55N are one order of magnitude higher
 316 than that of a marine diazotrophic cyanobacterium, *Crocospaera watsonii* strain WH8501 ($0.2\text{-}1.0 \times$
 317 $10^{-17} \text{ mol N} \times \text{cell}^{-1} \times \text{min}^{-1}$, $n = 4$) (cell = 2.5-6 μm in diameter), but they are only approximately
 318 half the rate of a marine diazotrophic cyanobacterium, *Trichodesmium erythraeum* ($19 \times 10^{-17} \text{ mol N}$
 319 $\times \text{cell}^{-1} \times \text{min}^{-1}$, $n = 1$) (cell = 6-22 μm wide \times approx. 10 μm long) (Tuit et al., 2004) (Table 2).
 320 Although the exact cell volumes of these microorganisms in the diazotrophic experiment were not
 321 directly measured, the results suggest that the nitrogen uptake rates per unit cell volume of these
 322 methanogens would be much higher than those of marine cyanobacteria (Table 2). The C/N molar
 323 ratios of Mc 1-85N and Mt 5-55N, respectively, ranged from 4.1 to 8.4 (generally 4.1 to 6.4) and 4.0
 324 to 7.3 (generally 4.1 to 5.5) under the various growth conditions.

325

326 3-2. Energetics of nitrogen fixation

327 The amount of CH_4 produced was linearly correlated with the amount of PN during the
 328 exponential growth of Mc 1-85N (Figure 2). The slope of the relationship between the amounts of
 329 CH_4 and PN represents the growth yield. The growth yield of Mc 1-85N under the diazotrophic
 330 condition was $36 \pm 3 \text{ mg N} \times (\text{mol CH}_4)^{-1}$ ($n = 11$) and was approximately one-fifth of that under the
 331 ammonium-replete condition (10 mM of NH_4^+) ($169 \pm 11 \text{ mg N} \times (\text{mol CH}_4)^{-1}$, $n = 5$). Interestingly,
 332 the growth yield of Mc 1-85N was $84 \pm 15 \text{ mg N} \times (\text{mol CH}_4)^{-1}$ when the ammonium concentration
 333 in the medium was below 200 μM ($n = 6$; data not shown). The growth yield of Mt 5-55N under the
 334 ammonium-replete condition was $170 \pm 40 \text{ mg N} \times (\text{mol CH}_4)^{-1}$ ($n = 3$).

335 During the exponential growth of Mc 1-85N, the potential energy yield from methanogenesis
 336 decreased from 132 to 92 $\text{kJ} \times (\text{mol CH}_4)^{-1}$ as H_2 concentration in the medium decreased from 1360

337 to 140 μM ($n = 8$; Table EA-1). In contrast, the constant growth yields of Mc 1-85N are consistent
338 with the observation that hydrogenotrophic methanogens generally produce the same number of ATP
339 per molecule of CH_4 generated, independent of the Gibbs energy change of methanogenesis (e.g.,
340 Thauer et al., 2008). The growth yield of Mc 1-85N under the diazotrophic condition is
341 higher-than-expected because, in theory, the number of ATP molecules needed for nitrogen fixation
342 is about ten times higher than that needed for ammonia assimilation (Cabello et al., 2009).

343

344 **3-3. Isotopic characteristics of nitrogen fixation and extracellular ammonium assimilation**

345 **3-3-1. Mc 1-85N**

346 Under the diazotrophic condition, the concentrations of PN and TN increased during growth
347 (Table 3). The concentrations of PN in the exponential phase (10, 12 and 16.5 h) were nearly equal to
348 those of TN within the analytical uncertainties. After 10 h, the $\delta^{15}\text{N}$ value of TN was constant at -4‰
349 (relative to the N_2 substrate) and was close to that of PN. The $\delta^{15}\text{N}$ (TN) value in the early growth
350 phase (2‰ at 6 h) was higher than that in the later growth phases. The $\delta^{15}\text{N}$ value of TN produced
351 during the growth of the methanogen ($\delta^{15}\text{N}$ (TN pro.)) was estimated from equation 3 to be -6.5‰
352 (relative to the N_2 substrate) for the period from 6 to 10 h. The $\delta^{15}\text{N}$ (TN pro.) value was -3.7‰ for
353 the period from 10 to 12 h and -4.5‰ for the period from 12 to 16.5 h (Table 3). The $\delta^{15}\text{N}$ values of
354 PN produced in the experiments were $-3.9 \pm 0.5\text{‰}$ (relative to the N_2 substrate) (1SD; $n = 48$) under
355 the various metal conditions (Figure 3a).

356 The positive $\delta^{15}\text{N}$ (TN) value at 6 h might be due to binary mixing of a ^{15}N -enriched
357 ammonium contaminant, initially present in the medium, with ^{15}N -depleted cellular nitrogen. The
358 mass contribution of the ammonium contaminant (70 ng N/mL) to TN was less than 12% at 6 h.
359 Hence, the $\delta^{15}\text{N}$ value of the ammonium contaminant should have been more than 42‰ (relative to
360 the N_2 substrate) if the $\delta^{15}\text{N}$ value of the cellular nitrogen was -4‰ (the same $\delta^{15}\text{N}$ value as the PN
361 after 10 h). Such a high $\delta^{15}\text{N}$ (NH_4^+) value seems to be unlikely because the $\delta^{15}\text{N}$ (NH_4^+) values of
362 the inoculum and the medium were likely less than NH_4Cl (+8.4‰; Section 2-4). Alternatively, the
363 $\delta^{15}\text{N}$ (TN) value at 6 h may be explained by the combination of a very small amount of isotopic
364 fractionation during nitrogen fixation in the early exponential phase and the presence of the
365 ammonium contaminant, which was slightly enriched in ^{15}N .

366 In the high-pressure experiments under the diazotrophic conditions, Mc 1-85N exhibited evident
367 growth, and the TN concentration increased from 0.2 to 46 $\mu\text{g N/mL}$ at the maximum (9 days after
368 inoculation). The $\delta^{15}\text{N}$ (TN pro.) value was $-3.9 \pm 0.9\text{‰}$ (1SD; $n = 5$) in the three independent
369 cultivations. No significant difference was observed for the $\delta^{15}\text{N}$ (TN pro.) values between the
370 high-pressure condition ($\text{H}_2 = 2 \text{ MPa}$, $\text{N}_2 = 2 \text{ MPa}$) and the normal pressure condition ($\text{H}_2 = 0.2 \text{ MPa}$,
371 $\text{N}_2 = 0.1 \text{ MPa}$) (Figure 3b).

372 By contrast, the magnitude of nitrogen isotope fractionation of ammonium uptake generally
373 decreased as the concentration of ammonium in the medium decreased. The $\epsilon_{\text{cell}/\text{NH}_4^+}$ value was $-16 \pm$
374 1‰ in a concentration range from 10 mM to 8 mM NH_4^+ ($f = 0.82\text{--}0.98$; $n = 4$), $-14 \pm 1\text{‰}$ in 1,070
375 to 670 $\mu\text{M NH}_4^+$ ($f = 0.78\text{--}0.87$; $n = 5$) and $-7 \pm 1\text{‰}$ in 200 to 70 $\mu\text{M NH}_4^+$ ($f = 0.58\text{--}0.76$; $n = 3$)
376 (Figure 4).

377

378 **3-3-2. Mt 5-55N**

379 Under the diazotrophic condition, the concentrations of PN and TN increased during growth
380 (Table 3). The concentration of PN in the exponential growth phase (16 h) was nearly equal to that of
381 TN, within the analytical uncertainty. The isotopic ratios of PN and TN were relatively constant
382 throughout growth. The $\delta^{15}\text{N}$ (TN pro.) value was -3.4‰ for the period from 13 to 16 h and -4.2‰
383 for the period from 16 to 26.5 h. The $\delta^{15}\text{N}$ values of PN produced in the experiments were $-3.7 \pm$
384 0.5‰ (1SD; $n = 17$) under the various metal conditions (Figure 3a). The $\epsilon_{\text{cell}/\text{NH}_4^+}$ value was $-17 \pm$
385 1‰ in a concentration range from 10 mM to 9 mM ($f = 0.92\text{--}0.99$; $n = 6$) (Figure 4).

386

387 **4. Discussion**

388 **4-1. Factors influencing isotopic fractionation during nitrogen fixation and intracellular** 389 **ammonia assimilation**

390 In the nitrogen fixation experiments, the concentrations of cellular nitrogen (i.e., PN) produced
391 were 1-10 $\mu\text{g N/mL}$, while those of ammonium initially present in the media were $\leq 70 \text{ ng N/mL}$.
392 The cellular nitrogen produced from the assimilation of the ammonium contamination could thus
393 alter the overall $\delta^{15}\text{N}$ (PN) values by $+1\text{‰}$ at the most, assuming that the $\delta^{15}\text{N}$ values of the
394 ammonium contamination are close to the NH_4Cl reagent (8.4‰, Section 2-4). Furthermore, the

395 amounts of N₂ consumed in diazotrophic cultivations were small (< 2% of the initial amounts of N₂).
396 The overall isotopic fractionations between PN and N₂ were thus estimated to be $-3.9 \pm 0.5\text{‰}$ (n =
397 48) and $-3.7 \pm 0.5\text{‰}$ (n = 17) for Mc 1-85N and Mt 5-55N, respectively, using equation 5.

398 The overall isotopic fractionations by the methanogens were larger than those of photosynthetic
399 prokaryotes ($-1.4 \pm 0.9\text{‰}$, n = 51; Minagawa and Wada, 1986; Macko et al., 1987; Carpenter et al.,
400 1997; Beaumont et al., 2000; Zerkle et al., 2008; Bauersachs et al., 2009) (Kruskal-Wallis, p-value <
401 0.001) (Figure 5). It is interesting to consider what factors may cause the differing amounts of overall
402 isotopic fractionation by methanogens and photosynthetic prokaryotes during nitrogen fixation and
403 cellular nitrogen assimilation. Nitrogen fixation consists primarily of a two-step process: the
404 diffusion of N₂ into the cell (step 1) and the reduction of N₂ to ammonia by nitrogenase in the
405 cytoplasm (step 2). Cellular nitrogen assimilation requires an additional step (step 3): the
406 assimilation of ammonia into cellular nitrogen compounds via glutamate and/or glutamine (Figure
407 A1-a). Several studies have shown that a certain fraction of the ammonia produced by nitrogenase is
408 not assimilated, but rather, it is excreted from diazotrophic cyanobacteria, leading to the formation of
409 a dissolved nitrogen pool (the sum of the dissolved organic nitrogen and dissolved inorganic nitrogen
410 other than N₂) in the surrounding environment (Glibert and Bronk 1994). Thus, the isotopic ratio of
411 PN reflects not only the isotopic fractionation of nitrogen fixation (ϵ_{step_1} , ϵ_{step_2}) but also that of
412 intracellular ammonia assimilation (ϵ_{step_3}) if the ammonia produced in step 2 is not entirely
413 converted to cellular nitrogen compounds. By contrast, the isotopic ratio of TN produced during
414 diazotrophy reflects the net isotopic fractionation of nitrogen fixation, not that of intracellular
415 ammonia assimilation.

416 In the exponential growth phases of Mc 1-85N and Mt 5-55N, TN was composed almost
417 completely (> 90%) of PN, and the $\delta^{15}\text{N}$ values of PN and TN represented rather similar values
418 (Table 3). Thus, the isotopic fractionation of intracellular ammonia assimilation (ϵ_{step_3}) is negligible,
419 and the difference between the isotopic ratios of PN and substrate N₂ should exactly represent the
420 isotopic fractionation of nitrogen fixation. Furthermore, the isotopic ratio of TN produced by Mc
421 1-85N was not affected by different concentrations of N₂ in the medium (380-7,600 μM ; Figure 3b),
422 suggesting that the isotopic fractionation effect during step 1 had little influence on the overall
423 isotopic fractionation. These results collectively indicate that the ¹⁵N-depleted cellular nitrogen of

424 methanogens primarily reflects an isotopic fractionation occurring during N₂ reduction by
 425 nitrogenase (ϵ_{step_2}).

426 The ϵ_{step_2} value did not vary with the different growth temperatures of the methanogens (55 and
 427 85 °C) or the different concentrations of Mo (5 nM–1 mM), Fe (100 nM–10 mM) and H₂ (up to 13
 428 mM). Isotopic fractionation during nitrogen fixation by the methanogens is thus predicted to be
 429 constant (-4‰) in natural hydrothermal environments that have broad gradients of temperature and
 430 metal concentrations due to the mixing of hot hydrothermal fluids and cold seawater.

431 The isotopically lighter cellular nitrogen of the methanogens likely results from a more negative
 432 ϵ_{step_2} value compared with the photosynthetic prokaryotes. Based on the phylogenetic distribution of
 433 nitrogenase gene sequences, the *Methanocaldococcus* and *Methanothermococcus* lineages are
 434 predicted to have nitrogenases with biochemically uncharacterised active site metal cofactors,
 435 whereas the photosynthetic prokaryotes have nitrogenases with FeMo-cofactors (Boyd et al., 2011a;
 436 Dos Santos et al., 2012). Our experiments suggest that the uncharacterised metal cofactors are not
 437 vanadium dependent because the culture media for the methanogens lacked vanadium. In contrast,
 438 our experiments suggest that Mt 5-55N requires molybdenum for the nitrogenase to function because
 439 the diazotrophic growth of Mt 5-55N was inhibited in a low Mo condition (Mo = 15 nM; Fe = 100
 440 μM ; H₂ = 0.2 MPa; N₂ = 0.1 MPa; NH₄⁺ < 10 μM), whereas it grew well with ammonium under a
 441 lower Mo condition (Mo = 5 nM; Fe = 100 μM ; H₂ = 0.2 MPa; N₂ not added; NH₄⁺ = 1 mM) (Table
 442 1). Mt 5-55N should thus contain Mo-bearing nitrogenase, consistent with the theoretical prediction
 443 that the uncharacterised active site metal cofactors are analogous to the FeMo-cofactor (McGlynn et
 444 al., 2013). The structural observation of the nitrogenase of Mt 5-55N is, however, required to
 445 demonstrate this inference. N₂ reduction to ammonia by the FeMo-cofactor is a multistep reaction
 446 via N_xH_y intermediates (Chatt et al., 1978; Seefeldt et al., 2009; Figure A1-b). The first step of N₂
 447 reduction possibly limits the overall rate of ammonia production because the triple bond of N₂ is
 448 highly stable (e.g., 948 kJ/mol in free state). The high stability of N₂ likely induces, to some extent,
 449 desorption of N₂ from the FeMo-cofactor, creating the following reaction flows: free N₂ (N≡N) ⇌
 450 N₂ adsorbed on the FeMo-cofactor (N≡N-Fe) → N_xH_y intermediates. Thus, the potential major
 451 factors influencing the ϵ_{step_2} value are the isotopic fractionations associated with forward and
 452 backward reactions of N≡N-Fe (i.e., reduction to NH=N-Fe and desorption, respectively) and a ratio
 453 of the forward and backward reaction flows (Rees 1973). Assuming the reduction steps of N₂ of the

454 uncharacterised active site metal cofactor are identical to those of the FeMo-cofactor, we expect the
 455 methanogens to have more negative ϵ_{step_2} values than photosynthetic prokaryotes in the following
 456 three cases:

- 457 i) when the magnitude(s) of isotopic fractionation(s) associated with forward and/or backward
 458 reaction(s) of N_2 on the uncharacterised cofactor is (are) larger than that on the FeMo-cofactor;
 459 ii) when the ratio of the forward and backward reaction flows of N_2 on the uncharacterised cofactor
 460 is different from the ratio on the FeMo-cofactor;
 461 iii) or a combined effect of i) and ii).

462 For further discussion, detailed information is required about local coordination of N_2 on the
 463 uncharacterised cofactor, and the kinetics of N_2 reduction steps and adsorption/desorption on the
 464 uncharacterised cofactor.

465

466 **4-2. Factors influencing isotopic fractionation during extracellular ammonium assimilation**

467 The apparent isotopic fractionations during extracellular ammonium assimilation of Mc 1-85N
 468 and Mt 5-55N under the ammonium-replete condition (10 mM of NH_4^+) were -16‰ and -17‰,
 469 respectively (Figure 4). These $\epsilon_{\text{cell}/\text{NH}_4^+}$ values of the methanogens are similar to those previously
 470 reported in bacteria grown under ammonium-replete conditions ($\epsilon_{\text{cell}/\text{NH}_4^+} = -15‰$ at 4–70 mM NH_4^+
 471 for *Anabaena vinelandii*, *Anabaena sp.* and *Vibrio harveyi*) (Delwiche and Steyn, 1970; Macko et al.,
 472 1987; Hoch et al., 1992). With a level of ammonium greater than several millimolar (> 3 mM)
 473 supplemented in a medium, *V. harveyi* used glutamate dehydrogenase to assimilate intracellular
 474 ammonium, primarily infiltrated as ammonia by membrane diffusion (Hoch et al., 1992).
 475 Consequently, the $\epsilon_{\text{cell}/\text{NH}_4^+}$ value of *V. harveyi* appears to represent the combined effects of the
 476 isotopic equilibrium between ammonium and ammonia and the kinetic isotope fractionation of
 477 glutamate dehydrogenase activity. By contrast, the methanogens likely use the GS-GOGAT pathway
 478 to assimilate intracellular ammonium, based on the genetic information of *Methanocaldococcus* and
 479 *Methanothermococcus* lineages (Table EA-2). Hence, the $\epsilon_{\text{cell}/\text{NH}_4^+}$ values of the methanogens under
 480 ammonium-replete conditions likely represent the combined effects of the isotopic equilibrium
 481 between ammonium and ammonia and the kinetic isotope fractionation of GS-GOGAT activity.

482 The $\epsilon_{\text{cell}/\text{NH}_4^+}$ value of Mc 1-85N increased from -14‰ to -7‰ with decreasing ammonium
483 concentrations in the medium from 1 mM to 100 μM (Figure 4). Similarly, an $\epsilon_{\text{cell}/\text{NH}_4^+}$ value of -4‰
484 has been reported in *V. harveyi* grown in a medium containing only 20 μM of NH_4^+ (Hoch et al.,
485 1992). The increase in the $\epsilon_{\text{cell}/\text{NH}_4^+}$ value of *V. harveyi* with decreasing ammonium concentrations is
486 mainly due to switching the extracellular ammonium uptake mechanism from passive membrane
487 diffusion to an active, inter-membrane transport (Hoch et al., 1992). Genes for a putative ammonium
488 transporter are identified in the genomes of *Methanocaldococcus* and *Methanothermococcus* lineages
489 (Table EA-2). The increased $\epsilon_{\text{cell}/\text{NH}_4^+}$ value of Mc 1-85N under the ammonium-depleted condition
490 would thus originate from a small magnitude of isotopic fractionation by active ammonium transport,
491 as predicted in the case of *V. harveyi*.

492

493 **4-3. Implications for the ecological roles and evolutionary physiology of diazotrophic** 494 **methanogens**

495 The differing growth responses of Mc 1-85N and Mt 5-55N to the transition metal
496 concentrations under the diazotrophic conditions may provide interesting insights into the ecological
497 significance and evolutionary physiology of these diazotrophic methanogens. For diazotrophic
498 growth, Mc 1-85N showed an apparently lower requirement of and higher tolerance to transition
499 metals (Mo = 5 nM–1 mM; Fe = 100 nM–10 mM) than did Mt 5-55N (Section 4-1). It remains
500 uncertain whether the different responses to the transition metal concentrations for diazotrophic
501 growth are due primarily to the differences in cellular physiology between the hyperthermophilic and
502 thermophilic *Methanococcales* lineages or due solely to the corresponding differences between the
503 Mc 1-85N and Mt 5-55N strains. Nevertheless, this result implies that diazotrophic primary
504 production of hyperthermophilic methanogens within *Methanococcales* may be more feasible in a
505 broad spectrum of seafloor and subseafloor environments associated with H_2 -rich crustal
506 hydrothermal activities.

507 The apparently lower Mo requirement of Mc 1-85N for diazotrophic growth is most likely
508 associated with the possible existence and function of a high Mo affinity of inter-membrane
509 transporter or channel proteins adapted to environments having very low concentrations of Mo. In
510 contrast, a high Mo tolerance has been shown in *Anabaena vinelandii*, and it was found that cellular

511 Mo homeostasis was achieved by both the regulation of the extracellular Mo uptake rate and the
512 storage of excess amounts of Mo by Mo-storage proteins (up to 100 μM) (Pienkos and Brill, 1981;
513 Bellenger et al., 2011). Thus, the high tolerance to transition metals, such as Mo and Fe, shown by
514 hyperthermophilic methanogens may be dependent on mechanisms similar to those found in *A.*
515 *vinelandii*.

516 The concentration of soluble iron (Fe^{2+}) in seawater may have decreased from 1-100 μM before
517 2.5 Ga to 1 nM today due to the progressive oxidation of the ocean (Holland 1973, 1984; Beukas and
518 Klein, 1990; Canfield 2005). In contrast, the iron concentrations of high-temperature ($> 250\text{ }^\circ\text{C}$)
519 hydrothermal fluids in the Precambrian ocean are still in question. The current consensus appears to
520 be that the high-temperature hydrothermal fluids in the Precambrian ocean had about the same range
521 of iron concentrations as those observed in modern hydrothermal systems (generally 1-20 mM) (e.g.,
522 Seyfried et al., 1991; Douville et al., 2002). In contrast, geological observations and hydrothermal
523 experiments suggest that reactions between basalt and CO_2 -rich seawater in high-temperature zones
524 ($> 250\text{ }^\circ\text{C}$) could have generated alkaline, iron-poor (1 μM) hydrothermal fluids at mid-ocean ridges
525 before 3 Ga (Shibuya et al., 2010; 2013a, b). In the latter model, the iron source of Archean banded
526 iron formations is considered to be acidic to neutral, iron-rich hydrothermal fluids generated by the
527 rock-dominant water/rock reactions expected in oceanic plateau/island arc settings (Shibuya et al.,
528 2013a). In either case, the potential range of iron concentrations in the hydrothermal mixing zones
529 ($50\text{-}120\text{ }^\circ\text{C}$) at the Precambrian mid-ocean ridges would fall within the iron concentration range that
530 allows diazotrophic growth of Mc 1-85N. Hyperthermophilic methanogens may thus have lived in
531 the hydrothermal mixing zones throughout Earth's history, without suffering from iron limitation or
532 iron toxicity.

533 Mo-depleted (less than 10 nM) habitats may be typical of the seafloor and subseafloor
534 environments associated with crustal hydrothermal circulation for the present-day Earth and even for
535 the hydrothermal and non-hydrothermal oceanic environments in the Precambrian Eon. In the
536 present-day oxic seawater, Mo dissolves as molybdate (MoO_4^{2-}), and its concentration is 110 nM
537 (Morris, 1975; Collier, 1985). By contrast, Mo concentrations in high-temperature ($> 300\text{ }^\circ\text{C}$),
538 H_2S -abundant fluids from two hydrothermal fields are reported to be 2-5 nM, likely due to the
539 precipitation of Mo sulphides (Kishida et al., 2004). The primary source of Mo in the present-day
540 ocean is riverine molybdate, generated by the oxidative dissolution of Mo sulphides in the

541 continental crust (Bertine and Turekian, 1973; Taylor and McLennan, 1995), suggesting that the Mo
542 concentrations in the Precambrian ocean under the limited to low O₂ levels of the atmosphere should
543 have been low. Based on the abundance of Mo in Precambrian shale, the Mo concentration in the
544 Precambrian ocean is roughly estimated to be less than 10 nM before 800 Ma (Scott et al., 2008).
545 Due to experimental limitations, this study did not examine diazotrophy of Mc 1-85N in the presence
546 of Mo below 5 nM. It should be noted, however, that the concentration of molybdate in our sulphidic
547 medium during the experiment was likely lower than that of total Mo (the sum of the dissolved and
548 insoluble forms of Mo in the medium), due to the precipitation of particle-reactive oxythiomolybdate
549 (Section 2-3). This finding implies diazotrophy of Mc 1-85N in the presence of molybdate below 5
550 nM, and it highlights the possible abundance and function of diazotrophy by hyperthermophilic
551 methanogens in the hydrothermal mixing zones of the Precambrian ocean.

552

553 **4-4. Implications for nitrogen sources of microbial communities in early Archean** 554 **hydrothermal environments**

555 The isotopic records in geological samples may imply the possible emergence and function of
556 nitrogen fixation by hyperthermophilic methanogens in early Archean hydrothermal environments
557 (Figure 6a). The isotopic ratio of the atmospheric N₂ that was dissolved in seawater and preserved in
558 fluid inclusions has been determined from various geological samples deposited during different ages,
559 and it has been found to be virtually constant during the past 3.5 Gyr (-2–0‰; Sano and Pillinger,
560 1991; Nishizawa et al., 2007). In contrast, ¹⁵N-depleted organic matter (as low as -6‰) is found in
561 early Archean cherts generally produced by deep-sea hydrothermal activities (Beaumont and Robert,
562 1999; Ueno et al., 2004). The slight ¹⁵N-depletion of the organic matter compared to N₂ is consistent
563 with nitrogen fixation in the ancient hydrothermal environments.

564 We should be aware that abiotic processes might have created some of the organic nitrogen
565 compounds in the early Archean. Experimental studies have shown that abiotic reactions create
566 organic nitrogen compounds (amides, amino acids and nitriles) under some hydrothermal conditions
567 (e.g., Hennet, et al., 1992; Yanagawa and Kobayashi 1992; Marshall 1994; Rushdi and Simoneit
568 2004; Huber and Wächtershäuser, 2006). However, it is still debatable whether the abiotic reactions
569 had quantitatively created the organic nitrogen compounds in natural hydrothermal systems in the

570 early Earth because the previous experimental studies had assumed geologically unusually high
571 concentrations of reactants (e.g., carbon monoxide, potassium cyanide, formic acid, oxalic acid, and
572 ammonium-salts) (Bada et al., 2007; Aubrey et al., 2009). Furthermore, the nitrogen isotopic
573 fractionations during these reactions (e.g., Fischer-Tropsch-type reactions and Strecker synthesis)
574 have not been investigated. Although we cannot eliminate the possibility of abiotic synthesis of
575 organic nitrogen compounds in natural hydrothermal environments, it is premature to assess the
576 abiotic origins of organic nitrogen compounds in Archean hydrothermal deposits.

577 In contrast, multiple lines of evidence have suggested that potential hyperthermophilic
578 methanogens were alive in such seafloor and subseafloor environments associated with hydrothermal
579 activities in the early Earth. In the Pilbara Craton, numerous silica vein intrusions are found in the
580 surrounding basaltic greenstones in the Dresser Formation, and they are interpreted as the remnants
581 of seafloor hydrothermal conduits at 3.5 Ga (Isozaki et al., 1997; Nijman et al., 1999; Van
582 Kraendonk et al., 2001). The silica veins contain a substantial amount of organic matter and putative
583 microfossils with a $\delta^{13}\text{C}$ of -36‰ and ^{13}C -depleted CH_4 (as low as -56‰) within primary fluid
584 inclusions (Ueno et al., 2001; 2004; 2006). The ^{13}C -depleted organic matter and the CH_4 indicate
585 potential activity of hyperthermophilic methanogens at 3.5 Ga, but they would not have been
586 produced from abiotic Fischer-Tropsch-type reactions because of the absence of effective catalysts
587 (native metals and magnetite) for the reactions during the silica vein formation (Ueno et al., 2004;
588 2006b; see an alternative view by Sherwood Lollar and McCollom, 2006). Thus, this evidence is
589 consistent with the inference that the ^{15}N -depleted organic matter (as low as -4‰ ; Ueno et al., 2004)
590 in the silica veins is also derived from possible hyperthermophilic methanogen populations.

591 The study of the primary fluid inclusions in the silica veins from the Dresser Formation has
592 shown that the isotopic ratio of N_2 was -3 to $+1\text{‰}$ (Nishizawa et al., 2007), which is a ratio
593 comparable to that of N_2 typically dissolved in deep-sea hydrothermal fluids on the present-day Earth
594 (de Ronde et al., 2011). Hence, the $\delta^{15}\text{N}$ values of the organic matter potentially produced from the
595 diazotrophy of hyperthermophilic methanogen populations are estimated from -7 to -3‰ , using the
596 $\delta^{15}\text{N}$ values of N_2 for the Archean hydrothermal fluids and the isotopic fractionation effect between
597 N_2 and cellular nitrogen compounds determined in this study (Figure 6b). Note that we cannot
598 directly compare the $\delta^{15}\text{N}$ values of the potential methanogen populations to those of the organic
599 matter in the silica veins.

600 The nitrogen compounds in sedimentary environments consist primarily of organic nitrogen
601 compounds and fixed ammonium. The fixed ammonium is a fraction of the ammonium released
602 from organic matter during diagenesis and subsequently fixed in clay minerals (Hall 1999). In
603 addition, during the metamorphic processes of the sedimentary rocks, the quantities and isotopic
604 ratios of the initial nitrogen compounds can change via thermal volatilisation (Hall 1999). Thus, to
605 correctly interpret the relationship between the nitrogen isotopic ratios of the initial organic
606 compounds in the past and the organic matter in the present, we must consider the possible isotopic
607 fractionations during diagenesis and metamorphism at different spatial and temporal scales.

608 The isotopic fractionation of metamorphism on sedimentary nitrogen compounds was evaluated
609 by stepwise combustion experiments of the silica veins from the Dresser Formation (Pinti et al., 2001,
610 2009). Based on an inverse relationship between the concentration and the isotopic ratio of nitrogen
611 released from the silica veins at temperatures above 500 °C, Pinti et al. (2009) estimated that the
612 $\delta^{15}\text{N}$ value of the pre-metamorphic sedimentary nitrogen in the silica veins had been between -7 and
613 -4‰.

614 In addition, the long-term (most likely, microbial and thermal) maturation of organic matter
615 during burial diagenesis would release ammonium and could alter the isotopic ratio. However,
616 previous studies have shown that the $\delta^{15}\text{N}$ values of ammonium (both the free and fixed forms) are
617 typically close to those of the bulk sedimentary nitrogen and organic matter ($\pm 1\%$; Williams et al.,
618 1995; Freudenthal et al., 2001; Prokopenko et al., 2006). These observations imply that burial
619 diagenesis would provide minimal isotope fractionation and that the ammonium released from the
620 source organic matter may have an isotopic ratio similar to that of the source organic matter, as much
621 as $\pm 1\%$.

622 In the early phase of deposition, organic matter is more or less influenced by the
623 decompositional functions of microbial communities (early diagenesis). Two types of microbial
624 decompositional processes are known to alter the $\delta^{15}\text{N}$ values of the initial organic matter. One
625 process is the microbial decomposition of organic matter under aerobic conditions, which typically
626 results in the ^{15}N enrichment of sedimentary nitrogen by +3 to +4‰ (Altabet and Francois, 1994;
627 Nakatsuka et al., 1997; Möbiuset al., 2010). The other process is the decomposition of organic matter
628 by anaerobic microbial populations, which typically leads to limited or slight ^{15}N depletion of
629 sedimentary nitrogen (-2 to 0‰) (Lehmann et al., 2002; Higgins et al., 2010; Möbiuset al., 2010). In

630 the case of the anoxic Archean ocean and hydrothermal environments, it is hypothesised that
631 anaerobic microbial decomposition caused the nitrogen isotopic alteration of the organic matter in
632 the silica veins during early diagenesis.

633 Based on our discussion of the possible isotopic alteration processes, such as metamorphism,
634 burial diagenesis and early diagenesis, we predict that the nitrogen isotopic ratios of the initial
635 organic matter at the time of vein formation in the Dresser Formation should range from -8 to -1‰
636 (i.e., $-7-1+0 = -8‰$, $-4+1+2 = -1‰$). This range is very similar to the estimated $\delta^{15}\text{N}$ range of the
637 organic compounds produced by the diazotrophic hyperthermophilic methanogens (-7 to -3‰).
638 Furthermore, N_2 is expected to be the predominant nitrogen compound in the hydrothermal fluids of
639 the Dresser Formation because the silica veins are thought to have been deposited in an Archean
640 mid-ocean ridge (Kitajima et al., 2001), implying ammonium-poor hydrothermal fluids with little
641 influence from sedimentary organic matter on the seafloor. Even if methanogens had assimilated tiny
642 amounts of ammonium, the $\delta^{15}\text{N}$ value of the resultant organic matter may have been lower than the
643 estimated $\delta^{15}\text{N}$ value of the initial organic matter (-8 to -1‰). This is because the isotopic ratio of
644 ammonium in the fluid inclusions is -10‰ (Nishizawa et al., 2007) and the assimilation of the
645 ammonium causes further ^{15}N depletion in the resultant organic matter ($< -10‰$; Figure 4). We
646 should note, however, that we could not entirely exclude the possibility of ammonium assimilation
647 by subpopulations of the potential microbial community in the Dresser hydrothermal environments.
648 Such a process may have caused a spread in $\delta^{15}\text{N}$ values of the initial organic matter toward -10‰.
649 However, nitrogen isotopic ratios of the organic matter in the Dresser silica veins require both the
650 presence of an initial organic matter whose $\delta^{15}\text{N}$ value is close to N_2 (-3 to +1‰) and the
651 involvement of nitrogen fixation in organic synthesis. We thus indicate the possible emergence and
652 function of diazotrophy by hyperthermophilic methanogens at 3.5 Ga.

653 Nitrogen fixation by ancient hyperthermophilic methanogens may have been conserved over the
654 long history of organic evolution. This conserved ability may be relevant to the ecological
655 significance of such methanogens in present-day oceanic hydrothermal systems. The ammonium
656 concentrations in the high temperature ($> 150\text{ }^\circ\text{C}$) fluids of typical basalt-hosted systems are low,
657 with values at 15 μM or less (German and Von Damm, 2003; Bourbonnais et al., 2012a). This
658 observation is consistent with the experimental results that suggest ammonium yields from abiotic N_2
659 reduction were low ($\leq 2.5\%$) under hydrothermal conditions (at 120-500 $^\circ\text{C}$ and 27-1000 bars in the

660 presence of magnetite, iron sulphides, iron metal, or nickel metal) (Brandes et al., 1998; Schoonen
661 and Xu, 2001; Smirnov et al., 2008). Thus, this substantial hydrothermal fluid chemistry has most
662 likely been unchanging over the history of the Earth. The low ammonia concentrations in the fluids
663 may have stimulated nitrogen fixation, as observed in methane seeps where ammonium
664 concentrations are 30-200 μM (Miyazaki et al., 2009; Dekas et al., 2013). Additionally, it is uncertain
665 whether substantial amounts of the nitrogen compounds originating from atmospheric chemistry
666 were transported to the ancient deep-sea hydrothermal systems, where they could persistently
667 support primary production by chemosynthetic microbial communities at a global scale. Nitric oxide,
668 hydrogen cyanide, and their decomposition products (nitrate, nitrite, and ammonium) are the
669 potential nitrogen products of the early atmosphere (Zahnle et al., 1986; Summers and Chang et al.,
670 1993; Navarro-González et al., 2001; Summers and Khare, 2007). Based on the kinetics of the
671 theoretical production/decomposition of ammonium and nitrite on the early Earth, Summers (1999)
672 suggested that ammonium concentrations in the early ocean were approximately 2 μM under various
673 temperature, pH and ferrous iron concentration conditions. In addition, the diazotrophic methanogens
674 of Mc 1-85N and Mt 5-55N lack the metabolic ability to utilise nitrate, a product of nitric oxide, as
675 the sole nitrogen source. In terms of the amount of elemental utilisation essential for the production
676 of substantial biomass, nitrogen fixation should have evolved, at least for these types of diazotrophic
677 methanogens and for any other microbial components of the ancient microbial ecosystems in the
678 ocean, at 3.5 Ga or even earlier.

679

680 **Acknowledgments**

681 We thank R. Senda and K. Suzuki for experimental assistance. We also thank T. Shibuya, K. Kawagucci, K.
682 Nakamura, J. Glass, and A. Kraepiel for fruitful discussion. Comments by T. McCollom and two anonymous
683 reviewers greatly improved the manuscript. This research was supported by the Ministry of Education, Culture,
684 Sports, Science and Technology of Japan (22540499 to M. N.).

685

686 **References**

- 687 Ader, M., Boudou, J., Javoy, M., Goffe, B. and Daniels, E. (1998) Isotope study on organic nitrogen of Westphalian
688 anthracites from the Western Middle field of Pennsylvania (U.S.A.) and from Bramsche Massif (Germany).
689 *Org. Geochem.* **29**, 315-323.
- 690 Ader, M., Cartigny, P., Boudou, J. P., Oh, J. H., Petit, E. and Javoy, M. (2006) Nitrogen isotopic evolution of

- 691 carbonaceous matter during metamorphism: Methodology and preliminary results. *Chem. Geol.* **232**, 152.
- 692 Altabet, M. A. and R. Francois (1994) Sedimentary nitrogen isotopic ratio as a recorder for surface ocean nitrate
693 utilization. *Global Biogeochem. Cycles* **8**, 103-116.
- 694 Aubrey, A. D., Cleaves, H. J. and Bada, J. L. (2009) The Role of Submarine Hydrothermal Systems in the
695 Synthesis of Amino Acids. *Origins Life Evol. Biospheres* **39**, 91-108.
- 696 Bada, J. L., Fegley, B., Miller, S. L., Lazcano, A., Cleaves, H. J., Hazen, R. M. and Chalmers, J. (2007) Debating
697 Evidence for the Origin of Life on Earth. *Science* **315**, 937-939.
- 698 Bauersachs, T., Schouten, S., Compaore, J., Wollenzien, U., Stal, L. J. and Damste, J. S. S. (2009) Nitrogen isotopic
699 fractionation associated with growth on dinitrogen gas and nitrate by cyanobacteria. *Limnol. Oceanogr.* **54**,
700 1403-1411.
- 701 Beaumont, V. and Robert, F. (1999) Nitrogen isotope ratios of kerogens in Precambrian cherts: a record of the
702 evolution of atmosphere chemistry. *Precam. Res.* **96**, 63-82.
- 703 Beaumont, V. I., Jahnke, L. L. and Des Marais, D. J. (2000) Nitrogen isotopic fractionation in the synthesis of
704 photosynthetic pigments in *Rhodobacter capsulatus* and *Anabaena cylindrica*. *Organic Geochem.* **31**,
705 1075-1085.
- 706 Bebout, G. E. and Fogel, M. (1992) Nitrogen-isotope compositions of metasedimentary rocks in the Catalina Schist,
707 California: implications for metamorphic devolatilization history. *Geochim. Cosmochim. Acta* **56**,
708 2839-2849.
- 709 Belay, N., Sparling, R. and Daniels, L. (1984) Dinitrogen fixation by a thermophilic methanogenic bacterium.
710 *Nature* **312**, 286-288.
- 711 Bellenger, J. P., Wichard, T., Xu, Y. and Kraepiel, A. M. L. (2011) Essential metals for nitrogen fixation in a
712 free-living N₂-fixing bacterium: chelation, homeostasis and high use efficiency. *Environ. Microbiol.* **13**,
713 1395-1411.
- 714 Bertine, K. K. and Turekian, K. K. (1973) Molybdenum in marine deposits. *Geochim. Cosmochim. Acta* **37**,
715 1415-1434.
- 716 Bethke, C. M. (2008) *Geochemical and Biogeochemical Reaction Modeling*. Cambridge, UK, Cambridge
717 University Press.
- 718 Beukes, N. J. and Klein, C. (1990) Geochemistry and sedimentology of a facies transition from microbanded to
719 granular iron-formation - In the early Proterozoic Transvaal Supergroup, South Africa. *Precam. Res.* **47**,
720 99-139.
- 721 Bourbonnais, A., Lehmann, M. F., Butterfield, D. A. and Juniper, S. K. (2012a) Subseafloor nitrogen
722 transformations in diffuse hydrothermal vent fluids of the Juan de Fuca Ridge evidenced by the isotopic
723 composition of nitrate and ammonium. *Geochem. Geophys. Geosyst.* **13**, doi:10.1029/2011GC003863.
- 724 Bourbonnais, A., Juniper, S. K., Butterfield, D. A., Devol, A. H., Kuypers, M. M. M., Lavik, G., Hallam, S. J., Wenk,
725 C. B., Chang, B. X., Murdock, S. A. and Lehmann, M. F. (2012b) Activity and abundance of denitrifying
726 bacteria in the subsurface biosphere of diffuse hydrothermal vents of the Juan de Fuca Ridge.
727 *Biogeosciences* **9**, 4661-4678.

- 728 Boyd, E. S., Hamilton, T. L. and Peters, J. W. (2011a) An alternative path for the evolution of biological nitrogen
729 fixation. *Frontiers Microbiol.* **2**. doi: 10.3389/fmicb.2011.00205
- 730 Boyd, E. S., Anbar, A. D., Miller, S., Hamilton, T. L., Lavin, M. and Peters, J. W. (2011b) A late methanogen origin
731 for molybdenum-dependent nitrogenase. *Geobiology* **9**, 221-232.
- 732 Brandes, J. A., Boctor, N. Z., Cody, G. D., Cooper, B. A., Hazen, R. M. and Yoder, H. S. (1998) Abiotic nitrogen
733 reduction on the early Earth. *Nature* **395**, 365-367.
- 734 Brandes, J. A., Hazen, R. M. and Yoder, H. S. (2008) Inorganic Nitrogen Reduction and Stability under Simulated
735 Hydrothermal Conditions. *Astrobiology* **8**, 1113-1126.
- 736 Butterfield, D. A., Roe, K. K., Lilley, M. D., Huber, J. A., Baross, J. A., Embley, R. W. and Massoth, G. J. (2004)
737 Mixing, reaction and microbial activity in the sub-seafloor revealed by temporal and spatial variation in
738 diffuse flow vents at Axial Volcano. In *the Subseafloor Biosphere at Mid-Ocean Ridges* (Eds. W. S. D.
739 Wilcock, E. F. DeLong, D. S. Kelley, J. A. Baross, and S. C. Cary) Geophys. Monogr. 144, Washington, D.
740 C, AGU, pp. 269–289.
- 741 Brandes, J. A. and Devol, A. H. (2002) A global marine-fixed nitrogen isotopic budget: Implications for Holocene
742 nitrogen cycling. *Global Biogeochem. Cycles* **16**, doi: 10.1029/2001GB001856
- 743 Cabello, P., Roldán, M. D., Castillo, F. and Moreno-Vivián, C. (2009) Nitrogen Cycle. In *Encyclopedia of*
744 *Microbiology (Third Edition)* (ed. S. Moselio) Academic Press, Oxford, pp. 299-321.
- 745 Calvert, S. E., Bustin, R. M. and Ingall, E. D. (1996) Influence of water column anoxia and sediment supply on the
746 burial and preservation of organic carbon in marine shales. *Geochim. Cosmochim. Acta* **60**, 1577-1593.
- 747 Canfield, D. E. (2005) The early history of atmospheric oxygen: Homage to Robert A. Garrels. *Annual Rev. Earth*
748 *Planet. Sci.* **33**, 1-36.
- 749 Carpenter, E. J., Harvey, H. R., Fry, B. and Capone, D. G. (1997) Biogeochemical tracers of the marine
750 cyanobacterium *Trichodesmium*. *Deep Sea Res. Part I: Oceanogr. Res.* **44**, 27-38.
- 751 Chatt, J., Dilworth, J. R., and Richards, R. L. (1978) Recent advances in the chemistry of nitrogen fixation.
752 *Chemical Reviews* **78**, 589-625.
- 753 Charlou, J. L., Fouquet, Y., Donval, J.P. and Auzende, J.M. (1996) Mineral and gas chemistry of hydrothermal
754 fluids on an ultrafast spreading ridge: East Pacific Rise, 17° to 19°S (Naudur cruise, 1993) phase separation
755 processes controlled by volcanic and tectonic activity. *J. Geophys. Res.* **101**, 15899–15919.
- 756 Charlou, J. L., Donval, J. P. and Douville, E. (2000) Compared geochemical signatures and the evolution of Menez
757 Gwen (37 degrees 50 ' N) and Lucky Strike (37 degrees 17 ' N) hydrothermal fluids, south of the Azores
758 Triple Junction on the Mid-Atlantic Ridge. *Chem. Geol.* **171**, 49-75.
- 759 Charlou, J. L., Donval, J. P., Fouquet, Y., Jean-Baptiste, P. and Holm, N. (2002) Geochemistry of high H₂ and CH₄
760 vent fluids issuing from ultramafic rocks at the Rainbow hydrothermal field (36°14'N, MAR). *Chem. Geol.*
761 **191**, 345-359.
- 762 Collier, R. W. (1985) Molybdenum in the northeast Pacific-ocean. *Limnol. Oceanogr.* **30**: 1351-1354.
- 763 Cowen, J. P., Giovannoni, S. J., Kenig, F., Johnson, H. P., Butterfield, D., Rappe, M. S., Hutnak, M. and Lam, P.
764 (2003) Fluids from aging ocean crust that support microbial life. *Science* **299**, 120-123.

- 765 de Ronde, C. E. J., Massoth, G. J., Butterfield, D. A., Christenson, B. W., Ishibashi, J., Ditchburn, R. G., Hannington,
766 M. D., Brathwaite, R. L., Lupton, J. E., Kamenetsky, V. S., Graham, I. J., Zellmer, G. F., Dziak, R. P.,
767 Embley, R. W., Dekov, V. M., Munnik, F., Lahr, J., Evans, L. J. and Takai, K. (2011) Submarine
768 hydrothermal activity and gold-rich mineralization at Brothers Volcano, Kermadec Arc, New Zealand.
769 *Mineralium Deposita* **46**, 541-584.
- 770 Dekas, A. E., Poretsky, R. S. and Orphan, V. J. (2009) Deep-Sea Archaea Fix and Share Nitrogen in
771 Methane-Consuming Microbial Consortia. *Science* **326**, 422-426.
- 772 Dekas, A. E., Chadwick, G. L., Bowles, M. W., Joye, S. B. and Orphan, V. J. (2013) Spatial distribution of nitrogen
773 fixation in methane seep sediment and the role of the ANME archaea. *Environ. Microbiol.* doi:
774 10.1111/1462-2920.12247
- 775 Delwiche, C. C. and Steyn, P. L. (1970) Nitrogen isotope fractionation in soils and microbial reactions. *Environ. Sci.*
776 *Technol.* **4**, 929-935.
- 777 Deming, J. W. and Baross J. A. (1993) Deep-sea smokers: Windows to a subsurface biosphere? *Geochim.*
778 *Cosmochim. Acta* **57**, 3219-3230.
- 779 Dos Santos, P., Fang, Z., Mason, S. and Setubal, J. (2012) Distribution of nitrogen fixation and nitrogenase-like
780 sequences amongst microbial genomes. *BMC Genomics* **13**, 162. doi:10.1186/1471-2164-13-162.
- 781 Douville, E., Charlou, J.L., Oelkers, E.H., Bienvenu, P., Jove Colon, C.F., Donval, J.P., Fouquet, Y., Prieur, D. and
782 Appriou, P. (2002) The rainbow vent fluids (36° 14'N, MAR): the influence of ultramafic rocks and phase
783 separation on trace metal content in mid-Atlantic ridge hydrothermal fluids. *Chem. Geol.* **184**, 37-48.
- 784 Erickson, B. E. and Helz, G. R. (2000) Molybdenum (VI) speciation in sulfidic waters: Stability and lability of
785 thiomolybdates. *Geochim. Cosmochim. Acta* **64**, 1149-1158.
- 786 Ferry, J. G. and House, C. H. (2006) The Stepwise Evolution of Early Life Driven by Energy Conservation.
787 *Molecular Biol. Evol.* **23**, 1286-1292.
- 788 Flores, G. E., Campbell, J. H., Kirshtein, J. D., Meneghin, J., Podar, M., Steinberg, J. I., Seewald, J. S., Tivey, M. K.,
789 Voytek, M. A., Yang, Z. K. and Reysenbach, A. L. (2011) Microbial community structure of hydrothermal
790 deposits from geochemically different vent fields along the Mid-Atlantic Ridge. *Environ. Microbiol.* **14**,
791 2158-2171.
- 792 Freudenthal, T., Wagner, T., Wenzhofer, F., Zabel, M., Wefer, G. (2001) Early diagenesis of organic matter from
793 sediments of the eastern subtropical Atlantic: Evidence from stable nitrogen and carbon isotopes. *Geochim.*
794 *Cosmochim. Acta* **65**, 1795-1808.
- 795 Furukawa, Y., Sekine, T., Oba, M., Kakegawa, T. and Nakazawa, H. (2009) Biomolecule formation by oceanic
796 impacts on early Earth. *Nature Geosci.* **2**, 62-66.
- 797 Garcia, J. L., Patel, B. K. C. and Ollivier, B. (2000) Taxonomic, Phylogenetic, and Ecological Diversity of
798 Methanogenic Archaea. *Anaerobe* **6**, 205-226.
- 799 Garvin, J., Buick, R., Anbar, A. D., Arnold, G. L. and Kaufman, A. J. (2009) Isotopic Evidence for an Aerobic
800 Nitrogen Cycle in the Latest Archean. *Science* **323**, 1045-1048.
- 801 German, C. R. and Von Damm, K. L. (2003) Hydrothermal processes. In *The Oceans and Marine Geochemistry*

- 802 (e.d. H. Elderfield) Vol. 6 *Treatise on Geochemistry* (eds. H. D. Holland, K. K. Turekian) Oxford,
803 Elsevier-Pergamon. pp. 181–222.
- 804 Glibert, P. M. and Bronk, D. A. (1994) Release of Dissolved Organic Nitrogen by Marine Diazotrophic
805 Cyanobacteria, *Trichodesmium* spp. *Appl. Environ. Microbiol.* **60**, 3996-4000.
- 806 Godfrey, L. V. and P. G. Falkowski (2009) The cycling and redox state of nitrogen in the Archean ocean. *Nature*
807 *Geosci.* **2**, 725-729.
- 808 Hall, A. (1999) Ammonium in granites and its petrographic significance. *Earth Sci. Rev.* **45**, 145-165.
- 809 Hamilton, T. L., Lange, R. K., Boyd, E. S. and Peters, J. W. (2011) Biological nitrogen fixation in acidic
810 high-temperature geothermal springs in Yellowstone National Park, Wyoming. *Environ. Microbiol.* **13**,
811 2204-2215.
- 812 Henet, R. J. C., Holm, N. G. and Engel, M. H. (1992) Abiotic synthesis of amino acids under hydrothermal
813 conditions and the origin of life: A perpetual phenomenon? *Naturwissenschaften* **79**, 361-365.
- 814 Hewson, I., Govil, S. R., Capone, D. C., Carpenter, E. J. and Fuhrman, J. A. (2004) Evidence of *Trichodesmium*
815 viral lysis and potential significance for biogeochemical cycling in the oligotrophic ocean. *Aquatic*
816 *Microbial Ecol.* **36**, 1-8.
- 817 Higgins, M. B., Robinson, R. S., Carter, S. J. and Pearson, Ann (2010) Evidence from chlorin nitrogen isotopes for
818 alternating nutrient regimes in the Eastern Mediterranean Sea. *Earth Planet. Sci. Letters* **290**, 102-107.
- 819 Hoch, M. P., Fogel, M. L. and Kirchman, D. L. (1992) Isotope fractionation associated with ammonium uptake by a
820 marine bacterium. *Limnol. Oceanogr.* **37**, 1447-1459.
- 821 Holland, H. D. (1984) *The Chemical Evolution of the Atmosphere and Oceans*. Princeton, NJ, Princeton Univ.
822 Press.
- 823 House, C. H., J. W. Schopf, J. W. and Stetter, K. O. (2003) Carbon isotopic fractionation by Archaeans and other
824 thermophilic prokaryotes. *Org. Geochem.* **34**, 345-356.
- 825 Huber, C. and Wächtershäuser, G. (2006) α -Hydroxy and α -Amino Acids Under Possible Hadean, Volcanic
826 Origin-of-Life Conditions. *Science* **314**, 630-632.
- 827 Huber, R., Wilharm, T., Huber, D., Trincone, A., Burggraf, S., König, H., Reinhard, R., Rockinger, I., Fricke, H.
828 and Stetter, K. O. (1992) *Aquifex pyrophilus* gen. nov. sp. nov., Represents a Novel Group of Marine
829 Hyperthermophilic Hydrogen-Oxidizing Bacteria. *Syst. Appl. Microbiol.* **15**, 340-351.
- 830 Isozaki, Y., Kabashima, T., Ueno, Y., Kitajima, K., Maruyama, S., Kato, Y. and Terabayashi, M. (1997) Early
831 Archean mid-oceanic ridge rocks and early life in the Pilbara Craton, W. Australia. *EOS* **78**, 399.
- 832 Jenkyns, H. C., Grocke, D. R. and Hesselbo, S. P. (2001) Nitrogen isotope evidence for water mass denitrification
833 during the early Toarcian (Jurassic) oceanic anoxic event. *Paleoceanogr.* **16**, 593-603.
- 834 Jia, Y. and Kerrich, R. (2004) Nitrogen 15-enriched Precambrian kerogen and hydrothermal systems. *Geochem.*
835 *Geophys. Geosyst.* **5**, Q07005, doi:07010.01029/02004GC000716.
- 836 Johnson, K. S., Childress, J. J., Hessler, R. R., Sakamoto-Arnold, C. M. and Beehler, C. L. (1988) Chemical and
837 biological interactions in the Rose Garden hydrothermal vent field, Galapagos spreading center. *Deep Sea*
838 *Res. Part A. Oceanogr. Res. Papers* **35**, 1723-1744.

- 839 Jones, W. J., Leigh, J. A., Mayer, F., Woese, C. R. and Wolfe, R. S. (1983) *Methanococcus jannaschii* sp. nov., an
840 extremely thermophilic methanogen from a submarine hydrothermal vent. *Archives of Microbiology* **136**,
841 254-261.
- 842 Junium, C. K. and M. A. Arthur (2007) Nitrogen cycling during the cretaceous, Cenomanian-Turonian oceanic
843 anoxic event II. *Geochem. Geophys. Geosys.* **8**, Q03002, doi: 10.1029/2006 gc001328.
- 844 Karl, D. M., Brittain, A. M. and Tilbrook, B. D. (1989) Hydrothermal and microbial processes at Loihi Seamount, a
845 mid-plate hot-spot volcano. *Deep Sea Res. Part A. Oceanogra.Res. Papers* **36**, 1655-1673.
- 846 Kishida, K., Sohrin, Y., Okamura, K. and Ishibashi, J. (2004) Tungsten enriched in submarine hydrothermal fluids.
847 *Earth and Planetary Science Letters* **222**, 819-827.
- 848 Kitajima, K., Maruyama, S., Utsunomiya, A. and Liou., J. G. (2001) Seafloor hydrothermal alteration at Archean
849 mid-ocean ridge. *Jour.Metamorphic Geol.* **19**, 583- 600.
- 850 Koba, K., Inagaki, K., Sasaki, Y., Takebayashi, Y. and Yoh, M. (2010) Nitrogen isotopic analysis of dissolved
851 inorganic and organic nitrogen in soil extracts. In *Earth, life and Isotopes* (eds. N. Ohkouchi, I. Tayasu and
852 K. Koba). Kyoto Univ. Press, Kyoto, Japan. pp. 17-36.
- 853 Kuypers, M. M. M., van Breugel, Y., Schouten, S., Erba, E. and Damste, J. S. S. (2004) N₂-fixing cyanobacteria
854 supplied nutrient N for Cretaceous oceanic anoxic events. *Geology* **32**, 853-856.
- 855 Lane, N. and Martin, W. F. (2012) The origin of membrane bioenergetics. *Cell* **151**, 1406-1416.
- 856 Lehmann, M. F., Bernasconi, S. M., Barbieri, A., McKenzie, J. A. (2002) Preservation of organic matter and
857 alteration of its carbon and nitrogen isotope composition during simulated and in situ early sedimentary
858 diagenesis. *Geochim. Cosmochim. Acta* **66**, 3573-3584.
- 859 Leigh, J. A. (2000) Nitrogen fixation in methanogens: the archaeal perspective. *Curr. Issues Mol. Biol.* **2**, 125-131.
860 Levman, B. G. and von Bitter, P. H. (2002)The Frasnian-Famennian (mid-Late Devonian) boundary in
861 the type section of the Long Rapids Formation, James Bay Lowlands, northern Ontario, Canada. *Canadian*
862 *Jour. Earth Sci.***39**, 1795-1818.
- 863 Macko, S. A., Fogel, M. L., Hare, P. E. and Hoering, T. C. (1987) Isotopic fractionation of nitrogen and carbon in
864 the synthesis of amino acids by microorganisms. *Chem. Geo.* **65**, 79-92.
- 865 Mariotti, A., Germon, J. C., Hubert, P., Kaiser, P., Letolle, R., Tardieux, A., Tardieux, P. (1981) Experimental
866 determination of nitrogen kinetic isotope fractionation. Some principles. Illustration for the denitrification
867 and nitrification processes. *Plant and Soil* **62**, 413-430.
- 868 Marshall, W. L. (1994) Hydrothermal synthesis of amino acids. *Geochim. Cosmochim. Acta* **58**, 2099-2106.
- 869 Martin, W. B., J., Kelley, D., Russell, M. J. (2008) Hydrothermal vents and the origin of life. *Nat. Rev. Microbiol.* **6**,
870 805-814.
- 871 McCollom, T. M. and Shock, E. L. (1997) Geochemical constraints on chemolithoautotrophic metabolism by
872 microorganisms in seafloor hydrothermal systems. *Geochim. Cosmochim. Acta* **61**, 4375-4391.
- 873 Mcglynn,S. E., Boyd,E. S., Peters,J. W. and Orphan,V. J (2013) Classifying the metal dependence of
874 uncharacterized nitrogenases. *Frontiers Microbiol.* **3**. doi: 10.3389/fmicb.2012.00419

- 875 Mehta, M. P. and J. A. Baross (2006) Nitrogen fixation at 92 degrees C by a hydrothermal vent archaeon. *Science*
876 **314**, 1783-1786.
- 877 Mehta, M. P., Butterfield, D. A. and Baross, J. A. (2003) Phylogenetic diversity of nitrogenase (nifH) genes in
878 deep-sea and hydrothermal vent environments of the Juan de Fuca ridge. *Appl. Environ. Microbiol.* **69**,
879 960-970.
- 880 Meyers, P. A. and Bernasconi, S. M. (2005) Carbon and nitrogen isotope excursions in mid-Pleistocene sapropels
881 from the Tyrrhenian Basin: Evidence for climate-induced increases in microbial primary production. *Mar.*
882 *Geol.***220**, 41-58.
- 883 Minagawa, M. and Wada, E. (1986) Nitrogen isotope ratios of red tide organisms in the East China Sea. A
884 characterization of biological nitrogen fixation. *Marine Chemistry* **19**, 245-259.
- 885 Mingram, B. and K. Bräuer (2001) Ammonium concentration and nitrogen isotope composition in metasedimentary
886 rocks from different tectonometamorphic units of the European Variscan Belt. *Geochim. Cosmochim. Acta*
887 **65**, 273-287.
- 888 Miyazaki, J., Higa, R., Toki, T., Ashi, J., Tsunogai, U., Nunoura, T., Imachi, H. and Takai, K. (2009) Molecular
889 Characterization of Potential Nitrogen Fixation by Anaerobic Methane-Oxidizing Archaea in the Methane
890 Seep Sediments at the Number 8 Kumano Knoll in the Kumano Basin, Offshore of Japan. *Appl. Environ.*
891 *Microbiol.* **75**, 7153–7162.
- 892 Möbius, J., Lahajnar, N. and Emeis, K. C. (2010) Diagenetic control of nitrogen isotope ratios in Holocene
893 sapropels and recent sediments from the Eastern Mediterranean Sea. *Biogeosciences* **7**, 3901-3914.
- 894 Morris, A. W. (1975) Dissolved molybdenum and vanadium in the northeast Atlantic Ocean. *Deep-Sea Res.***22**,
895 49-54.
- 896 Nakagawa, S., Takai, K., Horikoshi, K. and Sako, Y. (2003) *Persephonella hydrogeniphila* sp. nov., a novel
897 thermophilic, hydrogen-oxidizing bacterium from a deep-sea hydrothermal vent chimney. *Int. J. Syst. Evol.*
898 *Microbiol.***53**, 863-869.
- 899 Nakagawa, S., Takai, K., Inagaki, F., Horikoshi, K. and Sako, Y. (2005) *Nitratiruptor tergaricus* gen. nov., sp. nov.
900 and *Nitratifactor salsuginis* gen. nov., sp. nov., nitrate-reducing chemolithoautotrophs of the
901 ϵ -Proteobacteria isolated from a deep-sea hydrothermal system in the Mid-Okinawa Trough. *Int. J. Syst.*
902 *Evol. Microbiol.* **55**, 925-933.
- 903 Nakatsuka, T., Handa, N., Harada, N., Sugimoto, T. and Imaizumi, S. (1997) Origin and decomposition of sinking
904 particulate organic matter in the deep water column inferred from the vertical distributions of its $\delta^{15}\text{N}$, $\delta^{13}\text{C}$
905 and $\delta^{14}\text{C}$. *Deep Sea Res. Part I: Oceanogr. Res. Papers* **44**, 1957-1979.
- 906 Navarro-González, R., McKay, C. P. and Mvondo, D. N. (2001) A possible nitrogen crisis for Archaeal life due to
907 reduced nitrogen fixation by lightning. *Nature* **412**, 61-64.
- 908 Neuner, A., Jannasch, H. W., Belkin, S. and Stetter, K. O. (1990) *Thermococcus litoralis* sp. nov.: A new species of
909 extremely thermophilic marine archaeobacteria. *Archives Microbiol.***153**, 205-207.
- 910 Nijman, W., de Bruijne, K. H. and Valkering, M. E. (1999) Growth Fault control of early Archean cherts, barite

- 911 mound, and chert-barite veins, North Pole Dome, Eastern Pilbara, Western Australia. *Precam.Res.***95**,
912 247-274.
- 913 Nishizawa, M., Takahata, N., Terada, K., Komiya, T., Ueno, Y. and Sano, Y. (2005) Rare earth element, Lead,
914 Carbon and Nitrogen geochemistry of apatite-bearing metasediments from ~3.8 Ga Isua supracrustal belt,
915 West Greenland. *International Geol. Rev.***47**, 952-970.
- 916 Nishizawa, M., Sano, Y., Ueno, Y. and Maruyama, S. (2007) Speciation and isotope ratios of nitrogen in fluid
917 inclusions from seafloor hydrothermal deposits at ~3.5 Ga. *Earth Planet. Sci. Letters* **254**, 332-344.
- 918 Nishizawa, M., Koba, K., Makabe, A., Yoshida, N., Kaneko, M., Hirao, S., Ishibashi, J., Yamanaka, T., Shibuya, T.,
919 Kikuchi, T., Hirai, M., Miyazaki, J., Nunoura, T. and Takai, K. (2013) Nitrification-driven forms of nitrogen
920 metabolism in microbial mat communities thriving along an ammonium-enriched subsurface geothermal
921 stream. *Geochim. Cosmochim. Acta.* **113**, 152-173.
- 922 Ohkouchi, N., Kashiyama, Y., Kuroda, J., Ogawa, N. O. and Kitazato, H. (2006) The importance of diazotrophic
923 cyanobacteria as primary producers during Cretaceous Oceanic Anoxic Event 2. *Biogeosciences***3**,
924 467-478.
- 925 Orcutt, B. N., Bach, W., Becker, K., Fisher, A. T., Hentscher, M., Toner, B. M., Wheat, C. G. and Edwards, K. J.
926 (2011) Colonization of subsurface microbial observatories deployed in young ocean crust. *ISME J.* **5**,
927 692-703.
- 928 Papineau, D. M., S. J., Karhu, J. A. and Marty, B. (2005) Nitrogen isotopic composition of ammoniated
929 phyllosilicates: case studies from Precambrian metamorphosed sedimentary rocks. *Chem. Geol.* **216**,
930 37-58.
- 931 Papineau, D., Purohit, R., Goldberg, T., Pi, D. H., Shields, G. A., Bhu, H., Steele, A. and Fogel, M. L. (2009) High
932 primary productivity and nitrogen cycling after the Paleoproterozoic phosphogenic event in the Aravalli
933 Supergroup, India. *Precam. Res.* **171**, 37-56.
- 934 Pienkos, P. T. and Brill, W. J. (1981) Molybdenum accumulation and storage in *Klebsiella pneumoniae* and
935 *Azotobacter vinelandii*. *Jour. Bacteriol.***145**, 743-751.
- 936 Pinti, D. L., Hashizume, K. and Matsuda, J. (2001) Nitrogen and argon signatures in 3.8 to 2.8 Ga metasediments:
937 clues on the chemical state of the archaean ocean and the deep biosphere. *Geochim. Cosmochim. Acta* **65**,
938 2301-2315.
- 939 Pinti, D. L., Hashizume, K., Sugihara, A., Massault, M. and Philippot, P. (2009) Isotopic fractionation of nitrogen
940 and carbon in Paleoarchean cherts from Pilbara craton, Western Australia: Origin of N-15-depleted
941 nitrogen. *Geochim. Cosmochim. Acta***73**, 3819-3848.
- 942 Prokopenko, M. G., Hammond, D. E. and Stott, L. (2006) Lack of isotopic fractionation of ¹⁵N of organic matter
943 during long-term diagenesis in marine sediments; ODP Leg 202 – Sites 1234 and 1235. In *Proc. ODP, Sci.*
944 *Results, 202* (eds. R. Tiedemann, A. C. Mix., C. Richter, W. F. Ruddiman). ODP, pp. 1–22.
- 945 Raymond, J., Siefert, J. L., Staples, C. R. and Blankenship, R. E. (2004) The Natural History of Nitrogen Fixation.
946 *Mol. Biol. Evol.***21**, 541-554.

- 947 Rees, C. E. (1973) A steady-state model for sulphur isotope fractionation in bacterial reduction processes. *Geochim.*
948 *Cosmochim. Acta* **37**, 1141-1162.
- 949 Rushdi, A. I. and Simoneit, B. R. T. (2001) Lipid formation by aqueous Fischer-Tropsch-type synthesis over a
950 temperature range of 100 to 400°C. *Origins Life Evol. Biospheres* **31**, 103-118.
- 951 Russell, M. J., Hall, A. J. and Martin, W. (2010) Serpentinization as a source of energy at the origin of life.
952 *Geobiology* **8**, 355-371.
- 953 Russell, M. J. and W. Martin (2004) The rocky roots of the acetyl-CoA pathway. *Trends in Biochemical Sciences*
954 **29**, 358-363.
- 955 Sano, Y. and Pillinger, C. T. (1990) Nitrogen isotopes and N₂/Ar ratios in cherts: An attempt to measure time
956 evolution of atmospheric δ¹⁵N value. *Geochem. J.* **24**, 315-324.
- 957 Schoonen, M. A. A. and Xu, Y. (2001) Nitrogen Reduction Under Hydrothermal Vent Conditions: Implications for
958 the Prebiotic Synthesis of C-H-O-N Compounds. *Astrobiology* **1**, 133-142.
- 959 Scott, C., Lyons, T. W., Bekker, A., Shen, Y., Poulton, S. W., Chu, X. and Anbar, A. D. (2008) Tracing the stepwise
960 oxygenation of the Proterozoic ocean. *Nature* **452**, 456-459.
- 961 Seefeldt, L. C., Hoffman, B. M. and Dean, D. R. (2009) Mechanism of Mo-Dependent Nitrogenase. *Annual Rev.*
962 *Biochem.* **78**, 701-722.
- 963 Seyfried Jr, W. E., Ding, K. and Berndt, M. E. (1991) Phase equilibria constraints on the chemistry of hot spring
964 fluids at mid-ocean ridges. *Geochim. Cosmochim. Acta* **55**, 3559-3580.
- 965 Sherwood Lollar, B. S. and McCollom T. M. (2006) Geochemistry: Biosignatures and abiotic constraints on early
966 life. *Nature* **444**, E18-E18.
- 967 Shibuya, T., Komiya, T., Nakamura, K., Takai, K. and Maruyama, S. (2010) Highly alkaline, high-temperature
968 hydrothermal fluids in the early Archean ocean. *Precam. Res.* **182**, 230-238.
- 969 Shibuya, T., Yoshizaki, M., Masaki, Y., Suzuki, K., Takai, K. and Russell, M. J. (2013a) Reactions between basalt
970 and CO₂-rich seawater at 250 and 350°C, 500 bars: Implications for the CO₂ sequestration into the modern
971 oceanic crust and the composition of hydrothermal vent fluid in the CO₂-rich early ocean. *Chem. Geol.*
972 **359**, 1-9.
- 973 Shibuya, T., Tahata, M., Ueno, Y., Komiya, T., Takai, K., Yoshida, N., Maruyama, S. and Russell, M. J. (2013b)
974 Decrease of seawater CO₂ concentration in the Late Archean: an implication from 2.6 Ga seafloor
975 hydrothermal alteration. *Precam. Res.* **236**, 59-64.
- 976 Shock, E. L. and Holland, M. E. (2004) Geochemical Energy Sources that Support the Subsurface Biosphere. In *the*
977 *Subseafloor Biosphere at Mid-Ocean Ridges* (Eds. W. S. D. Wilcock, E. F. DeLong, D. S. Kelley, J. A.
978 Baross, and S. C. Cary) *Geophys. Monogr.* **144**, Washington, D. C, AGU, pp. 153-165.
- 979 Singireddy, S., Gordon, A. D., Smirnov, A., Vance, M. A., Schoonen, M. A. A., Szilagyi, R. K. and Strongin, D. R.
980 (2012). Reduction of Nitrite and Nitrate to Ammonium on Pyrite. *Origins Life Evol. Biospheres* **42**,
981 275-294.
- 982 Sleep, N. H. and Bird, D. K. (2007) Niches of the pre-photosynthetic biosphere and geologic preservation of Earth's

- 983 earliest ecology. *Geobiology* **5**, 101-117.
- 984 Smirnov, A., Hausner, D., Laffers, R., Strongin, D. R. and Schoonen, M. A. A. (2008) Abiotic ammonium
985 formation in the presence of Ni-Fe metals and alloys and its implications for the Hadean nitrogen cycle.
986 *Geochemical Transactions* **9** doi: 10.1186/1467-4866-9-5.
- 987 Solorzano, L. (1969) Determination of ammonia in natural waters by the phenol-hypochlorite method. *Limnol.*
988 *Oceanogr.* **14**, 799-801.
- 989 Steunou, A. S., Bhaya, D., Bateson, M. M., Melendrez, M. C., Ward, D. M., Brecht, E., Peters, J. W., Kuhl, M. and
990 Grossman, A. R. (2006) In situ analysis of nitrogen fixation and metabolic switching in unicellular
991 thermophilic cyanobacteria inhabiting hot spring microbial mats. *Proc. Natl. Acad. Sci. USA* **103**,
992 2398-2403.
- 993 Summers, D. (1999) Sources and Sinks for Ammonia and Nitrite on the Early Earth and the Reaction of Nitrite
994 with Ammonia. *Origins Life Evol. Biospheres* **29**, 33-46.
- 995 Summers, D. (2005) Ammonia Formation By The Reduction Of Nitrite/Nitrate By FeS: Ammonia Formation
996 Under Acidic Conditions. *Origins Life Evol. Biospheres* **35**, 299-312.
- 997 Summers, D. P. and Chang, S. (1993) Prebiotic ammonia from reduction of nitrite by iron (II) on the early Earth.
998 *Nature* **365**, 630-633.
- 999 Summers, D. and Khare, B. (2007) Nitrogen Fixation on Early Mars and Other Terrestrial Planets: Experimental
1000 Demonstration of Abiotic Fixation Reactions to Nitrite and Nitrate. *Astrobiology* **7**, 333-341.
- 1001 Summit, M. and Baross, J. A. (1998) Thermophilic seafloor microorganisms from the 1996 north Gorda Ridge
1002 eruption. *Deep Sea Res. Part II: Topical Studies Oceanogr.* **45**, 2751-2766.
- 1003 Takai, K. and Nakamura, K. (2011) Archaeal diversity and community development in deep-sea hydrothermal
1004 vents. *Curr. Opinion Microbiol.* **14**, 282-291.
- 1005 Takai, K. and Nakamura, K. (2010) Compositional, physiological and metabolic variability in microbial
1006 communities associated with geochemically diverse, deep-sea hydrothermal vent fluids. In
1007 *Geomicrobiology: Molecular and Environmental Perspective*. (eds. L. L. Barton, M. Mandl and A. Loy)
1008 Springer, pp. 251-283.
- 1009 Takai, K., Gamo, T., Tsunogai, U., Nakayama, N., Hirayama, H., Nealson, K. H. and Horikoshi, K. (2004)
1010 Geochemical and microbiological evidence for a hydrogen-based, hyperthermophilic subsurface
1011 lithoautotrophic microbial ecosystem (HyperSLiME) beneath an active deep-sea hydrothermal field.
1012 *Extremophiles* **8**, 269-282.
- 1013 Takai, K., Nakamura, K., Suzuki, K., Inagaki, F., Nealson K. H. and Kumagai, H. (2006)
1014 Ultramafics-Hydrothermalism-Hydrogenesis-HyperSLiME(UltraH³) linkage: a key insight into early
1015 microbial ecosystem in the Archean deep-sea hydrothermal systems. *Paleontological Res.* **10**, 269-282.
- 1016 Takai, K., Nakamura, K., Toki, T., Tsunogai, U., Miyazaki, M., Miyazaki, J., Hirayama, H., Nakagawa, S., Nunoura,
1017 T. and Horikoshi, K. (2008) Cell proliferation at 122°C and isotopically heavy CH₄ production by a
1018 hyperthermophilic methanogen under high-pressure cultivation. *Proc. National Aca. Sci. USA* **105**,
1019 10949-10954.

- 1020 Taylor, S. R. and McLennan, S. M. (1995) The geochemical evolution of the continental crust. *Rev. Geophys.* **33**,
1021 241–265.
- 1022 Thauer, R. K., Kaster, Anne-Kristin, Seedorf, H., Buckel, W. and Hedderich, R. (2008) Methanogenic archaea:
1023 ecologically relevant differences in energy conservation. *Nat. Rev. Microbiol.* **6**, 579-591.
- 1024 Thomazo, C., Ader, M. and Philippot, P. (2011) Extreme ¹⁵N-enrichments in 2.72-Gyr-old sediments: evidence for a
1025 turning point in the nitrogen cycle. *Geobiology* **9**, 107-120.
- 1026 Tivey, M. K. (2013) Environmental Conditions within Active Seafloor Vent Structures: Sensitivity to Vent Fluid
1027 Composition and Fluid Flow. In *the Subseafloor Biosphere at Mid-Ocean Ridges* (Eds. W. S. D. Wilcock,
1028 E. F. DeLong, D. S. Kelley, J. A. Baross, and S. C. Cary) *Geophys. Monogr.* **144**, Washington, D. C, AGU,
1029 pp. 137-152.
- 1030 Tuit, C., Waterbury, J. and Ravizzaz, G. (2004) Diel variation of molybdenum and iron in marine diazotrophic
1031 cyanobacteria. *Limnol. Oceanogr.* **49**, 978-990.
- 1032 Ueno, Y., Isozaki, Y., Yurimoto, H. and Maruyama, S. (2001) Carbon isotopic signatures of individual Archean
1033 microfossils (?) from Western Australia. *International Geol. Rev.* **43**, 196-212.
- 1034 Ueno, Y., Yoshioka, H., Maruyama, S. and Isozaki, Y. (2004) Carbon isotopes and petrography of kerogens in
1035 ~3.5-Ga hydrothermal silica dikes in the North Pole area, Western Australia. *Geochim. Cosmochim. Acta*
1036 **68**, 573-589.
- 1037 Ueno, Y., Yamada, K., Yoshida, N., Maruyama, S. and Isozaki, Y. (2006) Evidence from fluid inclusions for
1038 microbial methanogenesis in the early Archaean era. *Nature* **440**, 516-519.
- 1039 Ueno, Y., Yamada, K., Yoshida, N., Maruyama, S. and Isozaki, Y. (2006b) Geochemistry: Biosignatures and abiotic
1040 constraints on early life (Reply). *Nature* **444**, E18-E19.
- 1041 Van Kranendonk, M., Hickman, A. H., Williams, I. S. and Nijman, W. (2001) Archaean geology of the East Pilbara
1042 Granite-Greenstone Terrane, Western Australia - a field guide., Geological Survey of Western Australia.
- 1043 Ver Eecke, H. C., Butterfield, D. A., Huber, J. A., Lilley, M. D., Olson, E. J., Roe, K. K., Evans, L. J., Merkel, A.
1044 Y., Cantin, H. V. and Holden, J. F. (2012) Hydrogen-limited growth of hyperthermophilic methanogens at
1045 deep-sea hydrothermal vents. *Proc. National Aca. Sci. USA* **109**, 13674-13679.
- 1046 Wiesenburg, D. A. and Guinasso N. L. (1979) Equilibrium solubilities of methane, carbon monoxide, and hydrogen
1047 in water and sea water. *Jour. Chem. Engineering Data* **24**, 356-360.
- 1048 Williams, L. B., Ferrell, Jr. R. E., Hutcheon, I. Bakel, A. J., Walsh, M. M. and Krouse, H. R. (1995) Nitrogen
1049 isotope geochemistry of organic matter and minerals during diagenesis and hydrocarbon migration.
1050 *Geochim. Cosmochim. Acta* **59**, 765-779.
- 1051 Yanagawa, H. and Kobayashi, K. (1992) Chapter 8 An experimental approach to chemical evolution in submarine
1052 hydrothermal systems. *Origins Life Evol. Biospheres* **22**, 147-159.
- 1053 Zahnle, K. J. (1986) Photochemistry of methane and the formation of hydrocyanic acid (HCN) in the Earth's early
1054 atmosphere. *Jour. Geophysic. Res. Atmospheres* **91**, 2819-2834.
- 1055 Zerkle, A. L., Junium, C. K., Canfield, D. E. and House, C. H. (2008) Production of ¹⁵N-depleted biomass during

1056 cyanobacterial N₂-fixation at high Fe concentrations. *J. Geophys. Res. Biogeosci.* **113**, G03014,
1057 doi:03010.01029/02007JG000651.

1058

1059 **Figure legends**

1060 Figure 1: Growth curves of a) *Methanocaldococcus* sp. kairei 1-85N (Mc 1-85N) at 85 °C and b)
1061 *Methanothermococcus* sp. kairei 5-55N (Mt 5-55N) at 55 °C. Solid arrows in Figure 1a show the
1062 points of depletion of H₂ in the culture bottle. Except for a negative control experiment for Mc 1-85N
1063 at Fe = 1 mM, Mo = 100 nM, Ar = 0.1 MPa, CO₂ = 0.1 MPa and H₂ = 0.2 MPa, the initial partial
1064 pressures of N₂, CO₂ and H₂ in the headspace were set at 0.1 MPa, 0.1 MPa and 0.2 MPa,
1065 respectively.

1066

1067 Figure 2: a) Relationship between the amounts of CH₄ and particulate nitrogen during cultivation of
1068 Mc 1-85N at 85 °C. Error bars for the amounts of CH₄ and particulate nitrogen are smaller than the
1069 symbol sizes, except for the three points shown. b) Relationship between amounts of CH₄ and
1070 particulate carbon during cultivation of Mc 1-85N at 85 °C. Error bars for the amounts of CH₄ and
1071 particulate nitrogen are smaller than the symbol size, except for the three points shown. The symbols
1072 are the same as in Figure 1.

1073

1074 Figure 3: Stable nitrogen isotopic ratios of a) particulate nitrogen during the diazotrophic growth of
1075 Mc 1-85N and Mt 5-55N at a varying concentration of Mo in the medium under the atmospheric
1076 pressure condition, and b) total nitrogen produced during the diazotrophic growth of Mc 1-85N at
1077 various partial pressures of H₂ and N₂ in the media. In each graph, the second Y-axis (right side) is
1078 shown on a scale corresponding to the isotope enrichment factor of nitrogen fixation.

1079

1080 Figure 4: Nitrogen isotopic fractionation during extracellular ammonium uptake by Mc 1-85N and
1081 Mt 5-55N grown at different ammonium concentrations. Except for the results at the high
1082 ammonium concentration (10 mM), each symbol in the figure represents the result from a cultivation
1083 experiment. The isotope enrichment factor is plotted against the range of ammonium concentrations
1084 during each experiment.

1085

1086 Figure 5: Nitrogen isotopic ratios of cellular nitrogen compounds of diazotrophs relative to the
1087 substrate N₂. Data were obtained for non-heterocystous cyanobacteria from Carpenter et al. (1997)
1088 and Bauersachs et al. (2009) (square: *Lyngbya* sp.; star: *Crocospaera* sp.; diamond: *Cyanothece* sp.;
1089 inverted triangle: *Gloeothece* sp.; X: *Myxosarcina* sp.; filled circle: *Trichodesmium thiebautii*; open
1090 circle: *Trichodesmium* IMS101), for heterocystous cyanobacteria from Minagawa and Wada (1986),
1091 Macko et al. (1987), Beaumont et al. (2000), Zerkle et al. (2008) and Bauersachs et al. (2009)
1092 (square: *Anabaena variabilis*; star: *Anabaena cylindrica*; diamond: *Anabaena* sp. strain IF; inverted
1093 triangle: *Calothrix* sp.; X: *Nodularia* sp.; filled circle: *Nostoc* sp.) and for purple non-sulphur
1094 bacteria from Beaumont et al. (2000) (*Rhodobacter capsulatus*). Data for thermophilic and
1095 hyperthermophilic methanogens (average value ± standard deviation) are from this study.

1096

1097 Figure 6: Nitrogen isotopic ratios of a) various geological samples from different ages, and b)
1098 organic matter and fluid inclusions in the 3.5 Ga hydrothermal silica veins from the North Pole area
1099 in the Pilbara Craton, with the estimated range of nitrogen isotopic ratios of initial organic
1100 compounds at the time of deposition, and of cellular organic compounds produced by possible
1101 diazotrophic hyperthermophilic methanogens from hydrothermal fluid N₂ at that time. The isotopic
1102 range of the atmospheric N₂ during 3.5 Gyr is from Sano and Pillinger (1991) and Nishizawa et al.
1103 (2007). The nitrogen isotopic data of sedimentary rocks are from Calvert et al. (1996), Beaumont and
1104 Robert (1999), Jenkyns et al. (2001), Pinti et al. (2001), Levman and von Bitter (2002), Jia and
1105 Kerrich (2004), Kuypers et al. (2004), Ueno et al. (2004), Meyers and Bernasconi (2005), Nishizawa
1106 et al. (2005), Papineau et al. (2005), Ohkouchi et al. (2006), Junium and Arthur (2007), Garvin et al.
1107 (2009), Godfrey and Falkowski (2009), Papineau et al. (2009), Pinti et al. (2009) and Thomazo et al.
1108 (2011). In b), the nitrogen isotopic ratio data for organic matter and N₂ preserved in the 3.5 Ga
1109 hydrothermal silica veins are from Ueno et al., (2004) and Nishizawa et al., (2007).

1110

1111 Figure A1: a) A schematic illustration of nitrogen fixation and intracellular ammonia assimilation. b)
1112 A schematic illustration of postulated N₂ binding and reduction to NH₃ at an Fe site in the
1113 FeMo-cofactor of nitrogenase by limiting alternating (top) and distal (bottom) mechanisms proposed
1114 by Seefeldt et al. (2009) and Chatt et al. (1978), respectively.

Table 1: Growth characteristics of hyperthermophilic and thermophilic methanogens.

| Fe (nM) | Mo (nM) | NH ₄ ⁺ (μM) | NO ₃ ⁻ (μM) | N source(s) | μ (h ⁻¹) ^a | n ^b | Maximum cell yield (cell/ml) ^f |
|---|-----------|-----------------------------------|-----------------------------------|---|-----------------------------------|----------------|---|
| <i>Methanocaldococcus</i> sp. kairei 1-85N; T = 85 °C (This study) | | | | | | | |
| <i>H₂/CO₂/N₂ (50/25/25 mol%; 400 kPa)</i> | | | | | | | |
| 25 | 100 | <10 | <5 | N ₂ | – | 1 | NG |
| 100 | 5 | <10 | <5 | N ₂ | 0.31±0.07 | 3 | + |
| 100 | 100 | <10 | <5 | N ₂ | 0.27±0.01 | 4 | + |
| 100,000 | 1,000 | <10 | <5 | N ₂ | 0.32±0.03 | 4 | ++ |
| 100,000 | 100,000 | <10 | <5 | N ₂ | 0.23±0.01 | 7 | +++ |
| 1,000,000 | 15 | <10 | <5 | N ₂ | 0.29±0.05 | 3 | + |
| 1,000,000 | 100 | <10 | <5 | N ₂ | 0.26±0.01 | 4 | + |
| 1,000,000 | 1,000 | <10 | <5 | N ₂ | 0.29±0.01 | 3 | ++ |
| 1,000,000 | 10,000 | <10 | <5 | N ₂ | 0.28±0.02 | 7 | ++ |
| 1,000,000 | 1,000,000 | <10 | <5 | N ₂ | 0.32±0.09 | 3 | ++ |
| 10,000,000 | 10,000 | <10 | <5 | N ₂ | 0.17±0.02 | 4 | ++ |
| 10,000,000 | 100,000 | <10 | <5 | N ₂ | 0.31±0.02 | 3 | ++ |
| 10,000,000 | 1,000,000 | <10 | <5 | N ₂ | 0.12±0.01 | 5 | ++ |
| <i>H₂/CO₂/Ar (50/25/25 mol%; 400 kPa)</i> | | | | | | | |
| 1,000,000 | 100 | <10 | <5 | None | – | 1 | NG |
| 100,000 | 1,000 | 10,000 | <5 | NH ₄ ⁺ | 1.5±0.05 | 3 | +++ |
| 100,000 | 1,000 | <10 | 1000 | NO ₃ ⁻ | – | 2 | NG |
| <i>H₂/CO₂ (66/33 mol%; 300 kPa)</i> | | | | | | | |
| 100,000 | 5 | 1,000 | <5 | NH ₄ ⁺ | 0.81±0.12 | 6 | ++ |
| 100,000 | 1,000 | 10 | 100 | NH ₄ ⁺ , NO ₃ ⁻ | – | 2 | <1 x 10 ⁶ |
| 100,000 | 1,000 | <10 | 100 | NO ₃ ⁻ | – | 1 | NG |
| <i>Methanothermococcus</i> sp. kairei 5-55N; T = 55 °C (This study) | | | | | | | |
| <i>H₂/CO₂/N₂ (50/25/25 mol%; 400 kPa)</i> | | | | | | | |
| 100 | 100 | <10 | <5 | N ₂ | – | 2 | NG |
| 1,000 | 1,000 | <10 | <5 | N ₂ | – | 2 | NG |
| 10,000 | 1,000 | <10 | <5 | N ₂ | 0.25±0.01 | 4 | ++ |
| 10,000 | 10,000 | <10 | <5 | N ₂ | 0.26±0.01 | 3 | ++ |
| 100,000 | 15 | <10 | <5 | N ₂ | – | 2 | NG |
| 100,000 | 100 | <10 | <5 | N ₂ | – | 2 | NG |
| 100,000 | 1,000 | <10 | <5 | N ₂ | 0.29±0.05 | 4 | ++ |
| 100,000 | 10,000 | <10 | <5 | N ₂ | 0.29±0.02 | 4 | ++ |
| 100,000 | 100,000 | <10 | <5 | N ₂ | – | 2 | NG |
| 1,000,000 | 100 | <10 | <5 | N ₂ | – | 2 | NG |
| 1,000,000 | 10,000 | <10 | <5 | N ₂ | – | 2 | NG |
| 100,000 | 5 | 10,000 | <5 | NH ₄ ⁺ , N ₂ | – | 2 | ++ |
| 100,000 | 1,000 | 10,000 | <5 | NH ₄ ⁺ , N ₂ | 0.51±0.02 | 4 | ++ |
| 1,000,000 | 100 | 10,000 | <5 | NH ₄ ⁺ , N ₂ | – | 2 | NG |
| <i>H₂/CO₂/Ar (50/25/25 mol%; 400 kPa)</i> | | | | | | | |
| 100,000 | 1,000 | <0.01 | 1000 | NO ₃ ⁻ | – | 1 | NG |
| <i>H₂/CO₂ (66/33 mol%; 300 kPa)</i> | | | | | | | |
| 100,000 | 1,000 | 100 | 100 | NH ₄ ⁺ , NO ₃ ⁻ | – | 2 | + |
| 100,000 | 1,000 | 10 | 100 | NH ₄ ⁺ , NO ₃ ⁻ | – | 2 | NG |
| 100,000 | 5 | 1,000 | <5 | NH ₄ ⁺ | – | 2 | ++ |
| <i>Methanocaldococcus</i> FS406-22; T = 90 °C (Mehta and Baross, 2006) | | | | | | | |
| 5,500,000 | 4,800 | – | – | N ₂ | 0.22 | 3 | |
| 5,500,000 | 4,800 | 13,000 | 14,000 | NH ₄ ⁺ , NO ₃ ⁻ | 0.37 | 3 | |
| <i>Methanocaldococcus jannaschii</i>; T = 90°C (Jones et al., 1983) | | | | | | | |
| 10,000 | 410 | 5,000 | not added | NH ₄ ⁺ | 1.5 | 3 | |

a: Cell-based growth rate in exponential phase (mean ± standard deviation). -: Not measured.

b: Number of replicate determinations of the cell-based growth rate.

c: +++: (1-5) x 10⁸ cell/ml, ++: (1-10) x 10⁷ cell/ml, +: (1-10) x 10⁶ cell/ml, NG: No growth.

Table 2: Nitrogen uptake rates of diazotrophic microorganisms in exponential phase.

| Strain | Methanogen | | Cyanobacteria | | Soil bacteria |
|--|-----------------|-----------------|--------------------|-----------------|-------------------|
| | 1 | 2 | 3 | 4 | 5 |
| Nitrogen source | N ₂ | N ₂ | N ₂ | N ₂ | N ₂ |
| T [°C] | 85 | 55 | 28 | 28 | 22 |
| approximate cell volume [μm^3] ^a | 0.5-4 | 0.5-4 | 8-110 | 280-3800 | 0.5-4 |
| μ [h^{-1}] (cell-based) ^b | 0.27 \pm 0.04 | 0.25 \pm 0.02 | 0.01-0.02 | 0.02 | 0.25 ^h |
| Q _N [fmolN/cell] ^c | 6-24 | 18-22 | 7-30 | 529 | 17 ^h |
| ρN [10^{-17} molN/cell/min] ^d | 2-11 | 8 | 0.2-1 ^g | 19 ^g | 7 ^h |
| $\rho\text{N}'$ [10^{-17} μm^3 cell volume/min] ^e | 0.5-21 | 2-15 | 0.002-0.1 | 0.005-0.07 | 2-13 |
| N ^f | 7 | 2 | 4 | 1 | 1 |

Strain. 1: *Methanocaldococcus* sp. kairei 1-85N (This study); 2: *Methanothermococcus* sp. kairei 5-55N (This study); 3: *Crocospaera watonsonii* strain WH8501 (Tuit et al., 2004); 4: *Trichodesmium erythraeum* (Tuit et al., 2004); 5: *Azotobacter vinelandii* (Bellenger et al., 2011).

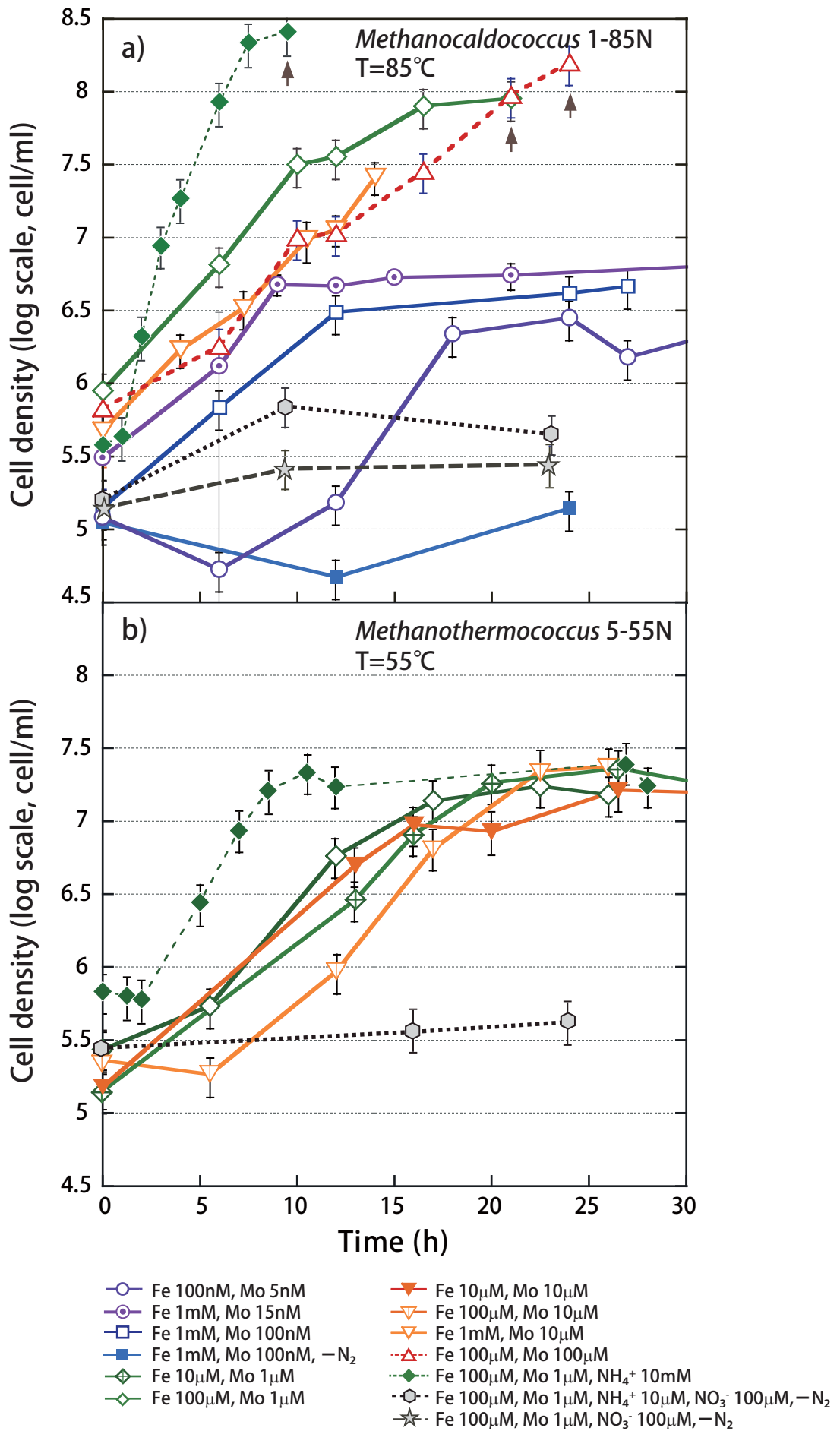
a. cell size of strain 1: 1-2 μm in diameter, 2: 1-2 μm in diameter, 3: 2.5-6 μm in diameter, 4: 6-22 μm wide \times 10 μm long, 5: 1-2 μm in diameter; **b.** Cell-based growth rate in exponential phase (mean \pm standard deviation); **c.** Cellular nitrogen content; **d.** Cell-based nitrogen uptake rate in exponential phase; **e.** Cell-based nitrogen uptake rate per unit cell volume calculated from ρN and approximate cell volume; **f.** Number of replicate determinations of μ ; **g.** The rate is estimated from daily-averaged cell-specific N assimilation rate; **h.** Maximum rate.

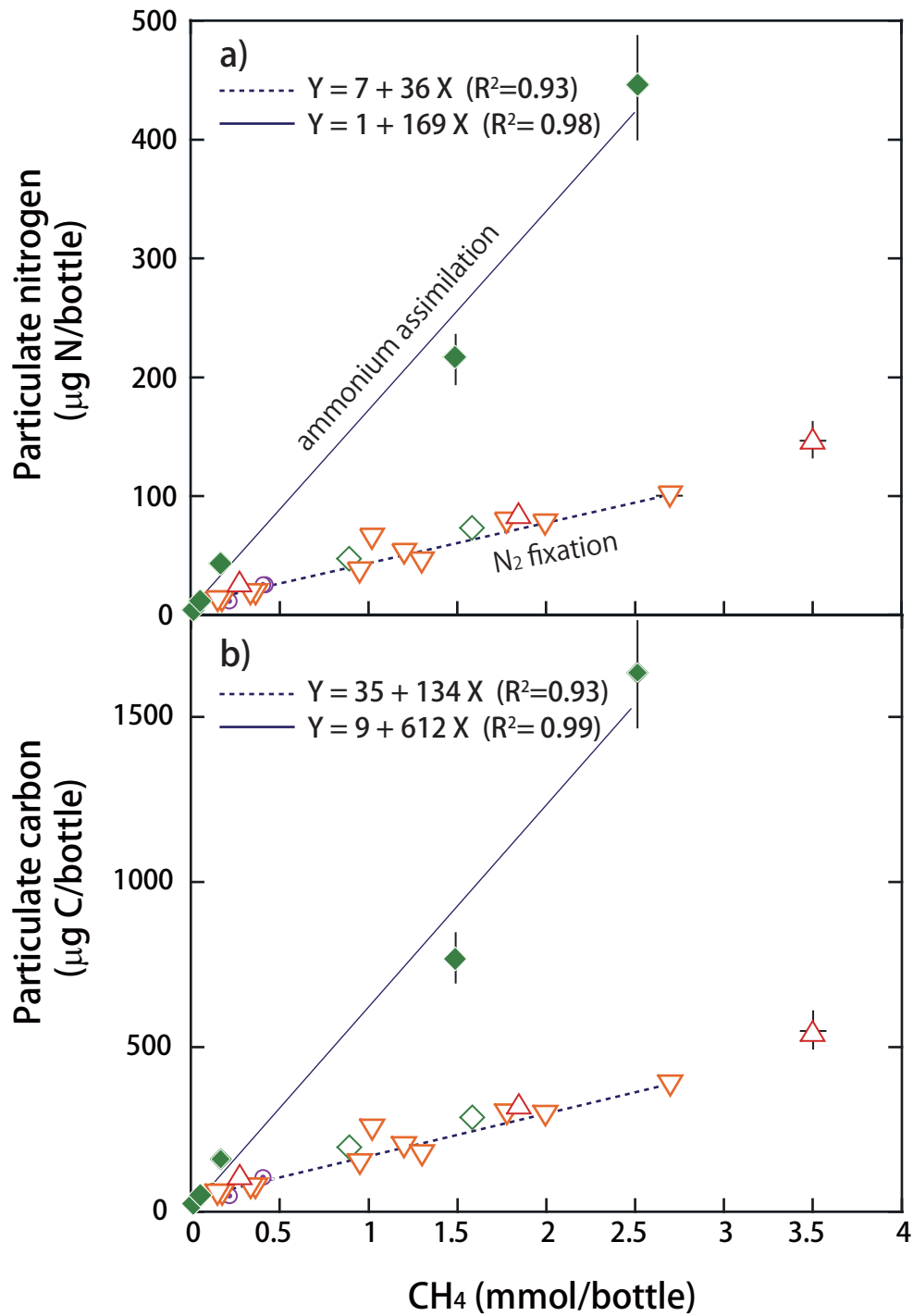
Table 3: Time course of concentrations and isotope ratios of particulate nitrogen compounds (PN) and total nitrogen (TN) during diazotrophic growth of methanogens.

| Time (h) | Cell density (cell/ml) | TN ^a (μg N/ml) | PN (μg N/ml) | δ ¹⁵ N (TN) ^a (‰) | δ ¹⁵ N (TN pro.) ^b (‰) | δ ¹⁵ N (PN) (‰) |
|---|------------------------|---------------------------|--------------|---|--|----------------------------|
| <i>Methanocaldococcus</i> sp. kairei 1-85N | | | | | | |
| T = 85 °C, Fe = 100,000 nM, Mo = 1000 nM, H ₂ /CO ₂ /N ₂ (50/25/25; 400 kPa) | | | | | | |
| 0 | 8.9 x 10 ⁵ | – | – | – | – | – |
| 6 | 6.6 x 10 ⁶ | 0.6 | – | 1.9 | – | – |
| 10 | 3.2 x 10 ⁷ | 2.3 ± 0.3 | 2.4 | –4.1 ± 0.4 | –6.5 ± 0.7 (6 ~ 10 h) | –4.4 |
| 12 | 3.6 x 10 ⁷ | 3.8 ± 0.5 | 3.7 | –4.0 ± 0.7 | –3.7 ± 0.2 (10 ~ 12 h) | –4.2 |
| 16.5 | 8.0 x 10 ⁷ | 11.3 ± 1.1 | 9.5 | –4.3 ± 0.5 | –4.5 ± 0.1 (12 ~ 16.5 h) | –4.3 |
| 21 | 9.1 x 10 ⁷ | – | 8.1 | – | – | –4.3 |
| <i>Methanothermococcus</i> sp. kairei 5-55N | | | | | | |
| T = 55 °C, Fe = 10,000 nM, Mo = 1000 nM, H ₂ /CO ₂ /N ₂ (50/25/25; 400 kPa) | | | | | | |
| 0 | 1.4 x 10 ⁵ | – | – | – | – | – |
| 13 | 2.9 x 10 ⁶ | 0.8 | – | –4.5 | – | – |
| 16 | 8.2 x 10 ⁶ | 2.1 | 2.5 | –3.8 | –3.4 ± 0.1 (13 ~ 16 h) | –3.7 |
| 26.5 | 2.3 x 10 ⁷ | 4.7 | 4.3 | –4.0 | –4.2 ± 0.1 (16 ~ 26.5 h) | –3.4 |
| 30.5 | 1.8 x 10 ⁷ | – | 4.1 | – | – | –3.4 |
| 48 | 3.2 x 10 ⁷ | – | 4.7 | – | – | –3.1 |

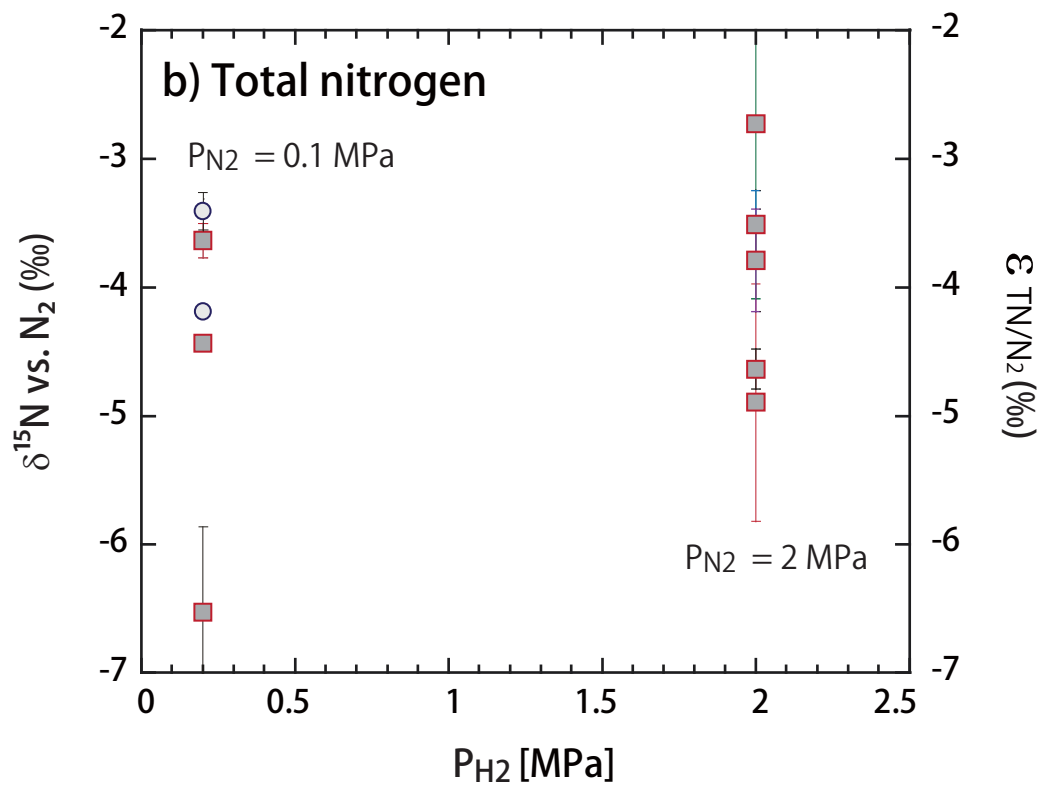
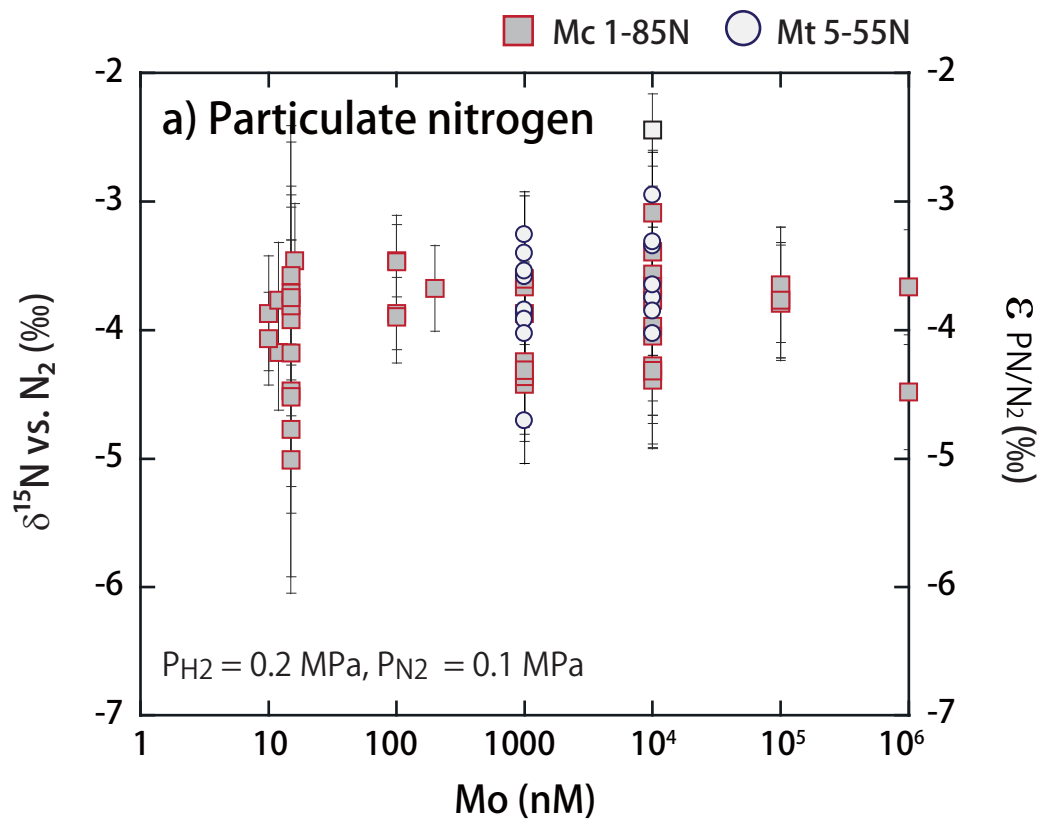
δ¹⁵N (TN), δ¹⁵N (TN pro.), and δ¹⁵N (PN) values are expressed relative to N₂ substrate in cultivation bottle, respectively.

a. Uncertainty shows standard deviation of duplicate or triplicate measurements; **b.** δ¹⁵N (TN pro.) denotes isotopic ratio of TN produced during growth, and is estimated by following equation: $\delta^{15}\text{N (TN pro.)} = ([\text{TN}] * \delta^{15}\text{N (TN)} - [\text{TN}]' * \delta^{15}\text{N (TN)'}) / ([\text{TN}] - [\text{TN}]')$. Symbols [TN] and [TN]' denote concentrations of TN at T and T' hours after cultivation starts (T > T').

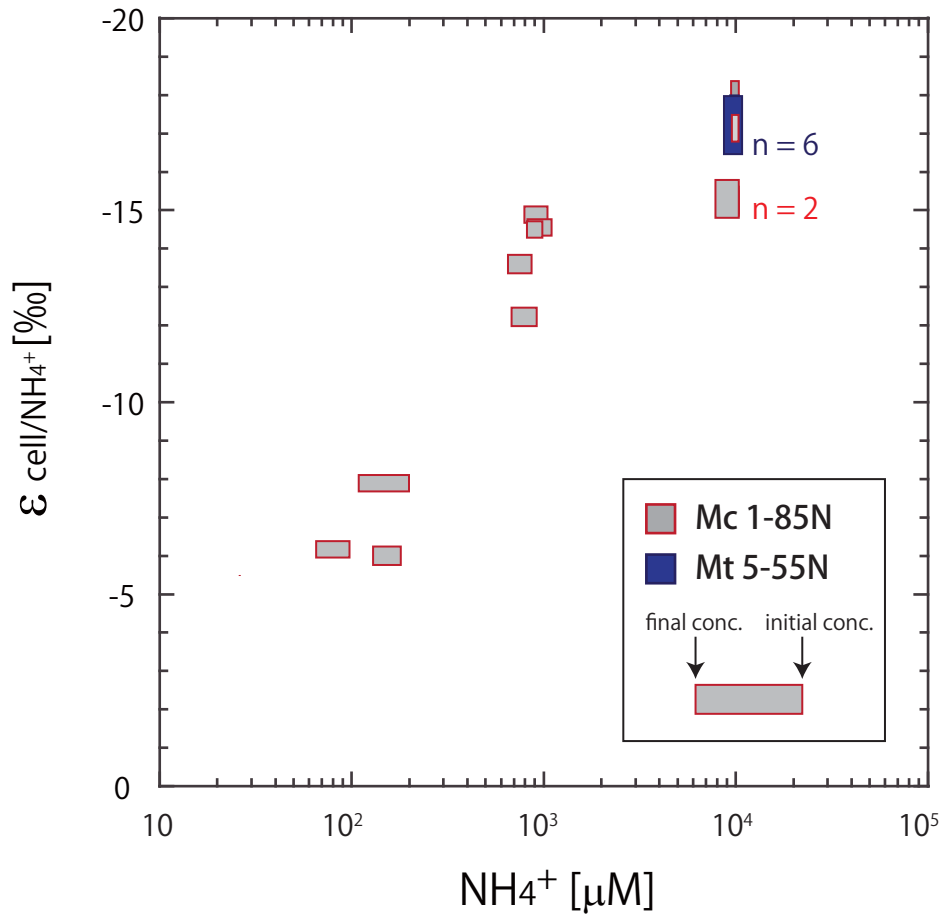


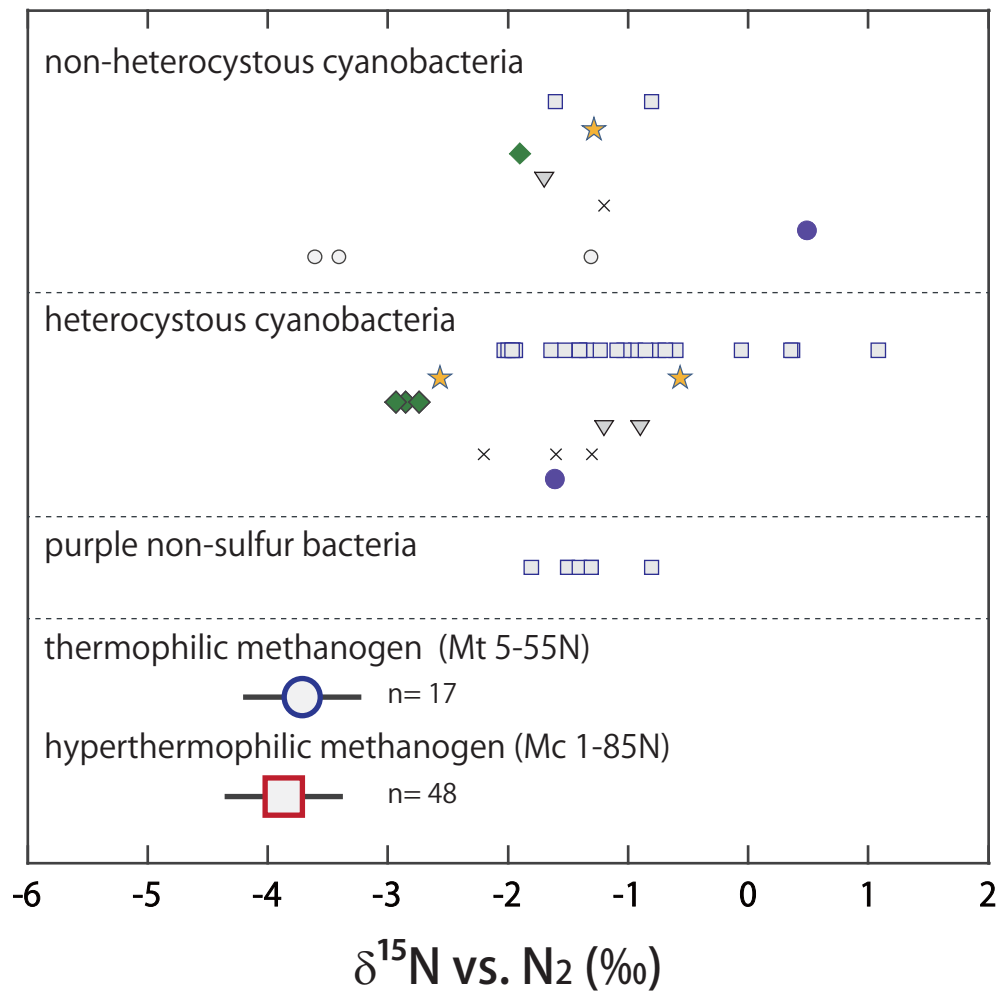


Nishizawa et al., Fig. 2

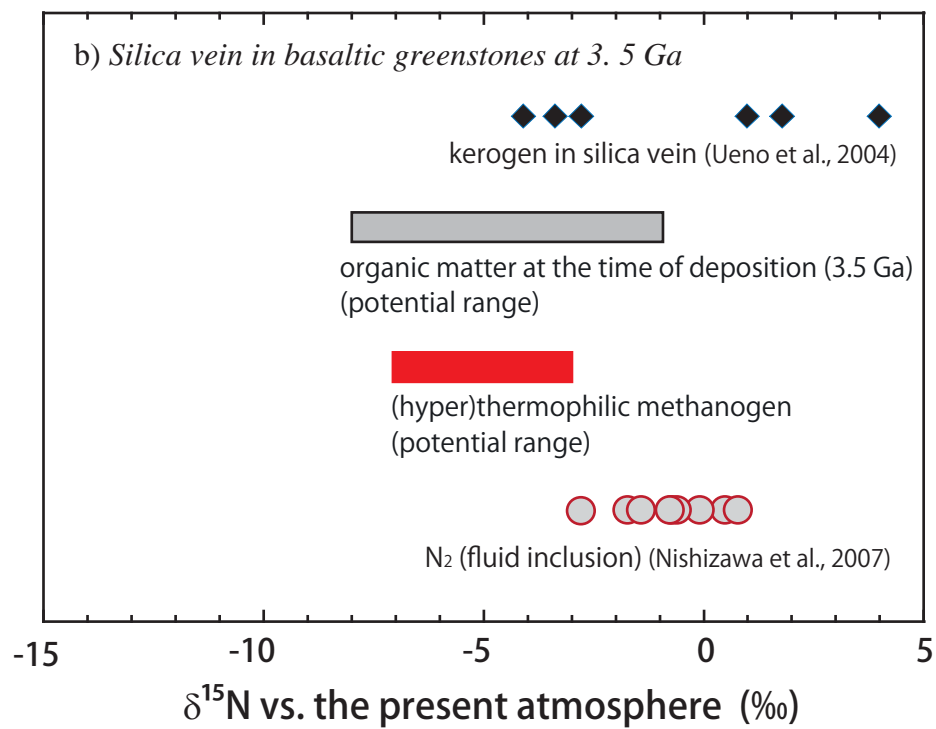
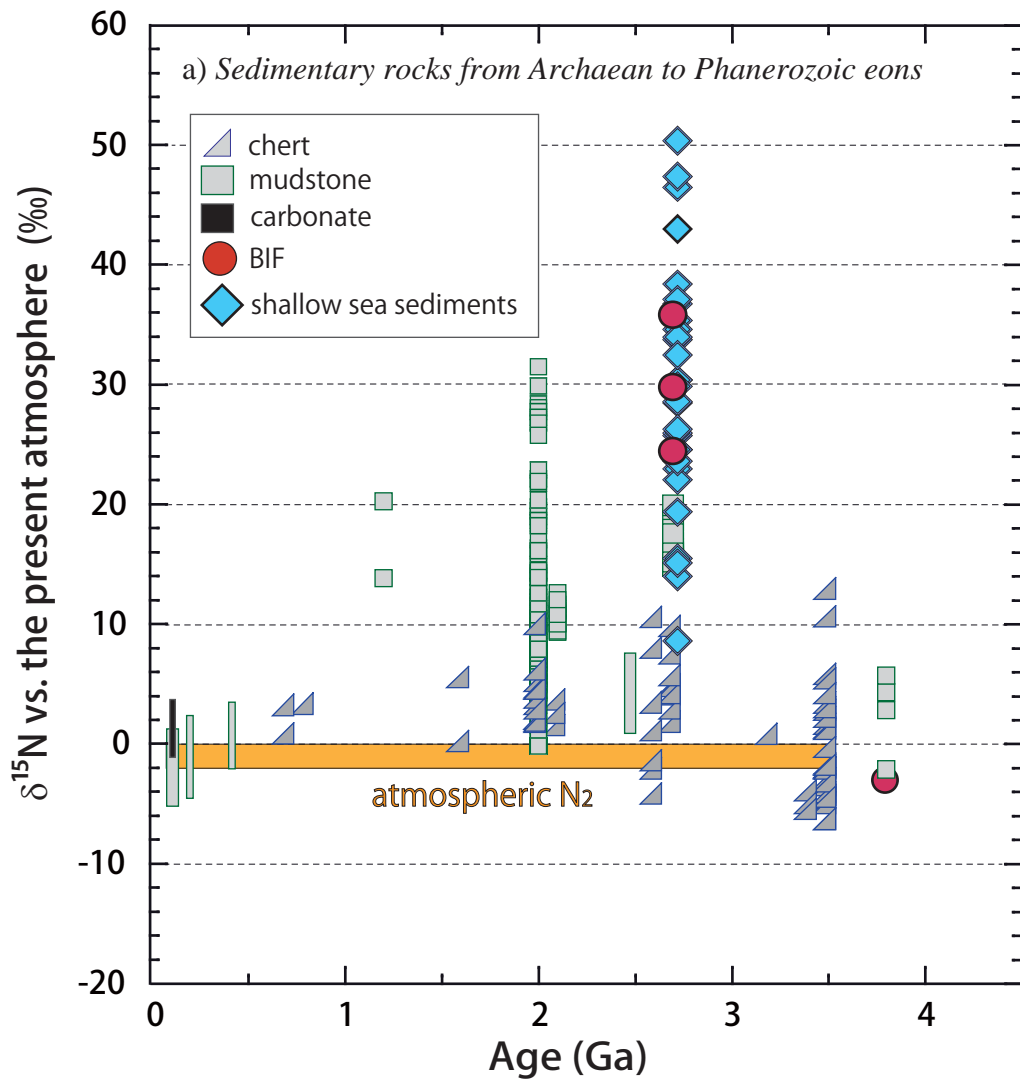


Nishizawa et al., Fig. 3

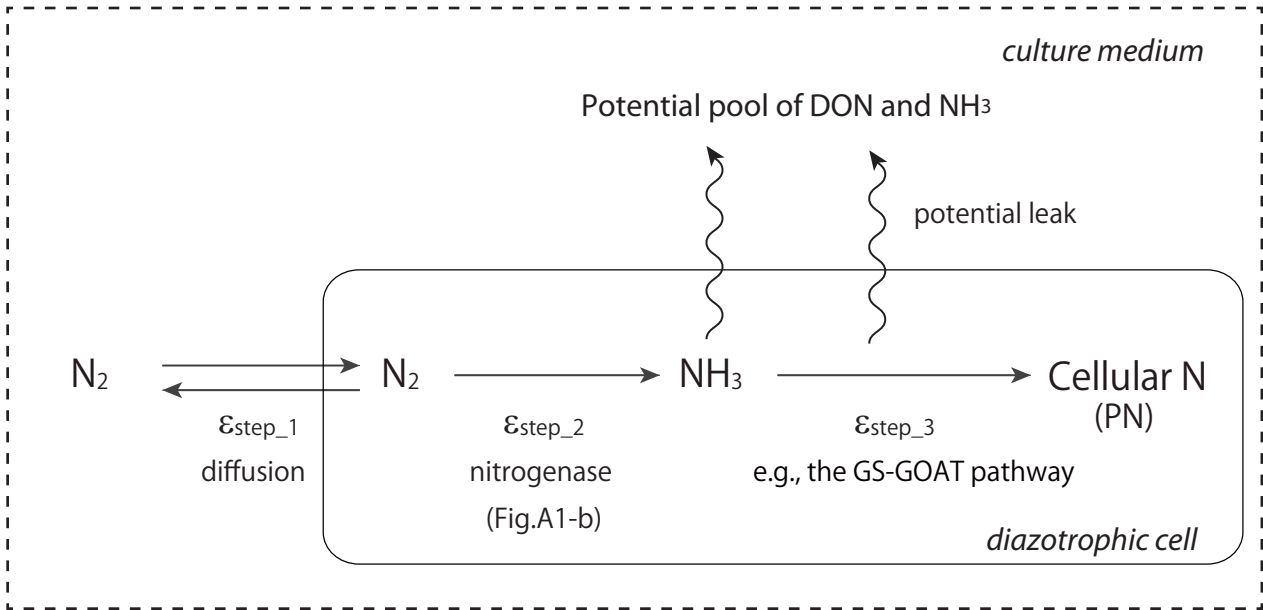




Nishizawa et al., Fig. 5



a) N₂ fixation and intracellular ammonia assimilation



Isotopic measurements

Particulate Nitrogen (PN) = Cellular N, Total Nitrogen (TN) = cellular N+DON+NH₃

b) N₂ binding and reduction to NH₃ at an Fe site in the FeMo cofactor of nitrogenase

